CHAPTER

31 Composite materiomics: Multi length scale hierarchical composites for structural and tissue engineering applications

Josef Jancar
Brno University of Technology, Brno, Czech Republic

31.1 INTRODUCTION

Historical advancement of human society has always been closely related to the level of sophistication of the available materials and manufacturing processes. A fundamental difference between synthetic materials and naturally formed biological materials is that functionality in biology can be created by arranging universal nanoscale building blocks (NSBBs) in different patterns, rather than by inventing new types of NSBBs, as in many synthetic materials [1,2]. Nature assembles hierarchical composite superstructures such as bones, teeth, cytoskeletons, wood, or silk fibers capable of function specific combination of properties, from NSBBs consisting of very limited number of constituents and performing specific functions at hierarchically arranged structural levels. Nature's growth process is based on synthesis of desired NSBBs followed by their *self-assembly (SA)* into superstructures with locally variable design constantly responding to external stimuli (T, pH, electric field, mechanical forces, etc.) [3–6]. The formation of hierarchical arrangements provides the structural basis to enable the existence of universality and diversity within a single superstructure [1,2].

Current *top-down* artificial composite design paradigm does not provide means to achieve hierarchical functional composite structures that can adapt independently while befitting a range of functions. Novel *bottom-up* material platform needs to be developed capable of adding *end-use specific functions* to their ever enhancing physicochemical properties and environmental friendliness. Fabricating functional composite superstructures, emulating the structural and functional hierarchy of load-bearing biocomposites, requires exquisite control over the development of the structural hierarchy. This can be achieved efficiently by employing combination of *SA* of NSBBs, with precise supramolecular architecture, into micron scale subunits

Multifunctionality of Polymer Composites. ISBN: 978-0-323-26434-1
DOI: http://dx.doi.org/10.1016/B978-0-323-26434-1.00031-3

with *commanded assembly* of these subunits into 3D macroscopic hierarchical structures [7–9]. It has to extend beyond biomimetics and bioinspired systems exploiting fundamental mechanisms of *SA* and hierarchies, and integrate *de novo* synthetized NSBBs. Answering the challenge of utilizing universal NSBBs to create diverse multifunctional hierarchical macroscopic superstructures that span to the nanoscale could enable the emergence of novel technological paradigm. The future artificial composite superstructures should be able to emulate the structural and functional hierarchy of load-bearing biocomposites while maintaining substantially shorter production period compared to growth.

To identify novel light weight, environmentally friendly engineering material platforms, a greater understanding must be achieved of the fundamental links between NSBB syntheses, hierarchical structure assembly, properties and functions at multiple length *and* time scales. In analogy to *genomics* investigating *genome*, *materiomics* [1] is an emerging interdisciplinary field investigating material in the complexity of its structure–property–function relationships (*materiome*). This interdisciplinary approach is based on an integration of concepts and techniques from engineering, material science, structural biology, chemistry, and physics in the context of developing novel material platforms with potential implications for nanotechnology and nanoscience.

Quantification of the structure–property relationships and understanding the multiscale *bottom-up* assembly processes is pivotal for both furthering our knowledge base and for the development of novel, efficient technologies to manufacture intelligent hierarchical polymer composites for use in engineering structures, tissue engineering, sensing, and photovoltaics. This requires design and execution of critical experiments providing unbiased reliable structure and property data, almost not present in the current literature, to reconsider classical theoretical framework of polymer physics failing to describe nanoscale phenomena. A comprehensive theoretical framework in which one can understand nanoparticle *SA* in the presence of polymer chains and the resulting effects on material properties is desired. We believe that the integration of length scales, as well as the mixing of physical, biological, and chemical concepts into tailoring properties of the hierarchical polymer superstructures in the process of their preparation could greatly advance the way we will design future smart materials. We also see a great challenge for science to discover natural laws governing structure–property relationships in superstructures hierarchically assembled from nanostructured building blocks over multiple length and time scales and employing this knowledge in design of smart materials for structural and biomedical applications. As a result, the field will likely be a fertile ground for investigation for many years to come.

31.2 *MATERIOMICS*: INVESTIGATING HIERARCHICAL MULTIFUNCTIONAL COMPOSITE STRUCTURES

In analogy to *genomics* investigating *genome*, *materiomics* is a new emerging interdisciplinary field investigating a given material in the complexity of its

structure–property–function relationships (*materiome*) [2–4]. At this time, *materiomics* research is mainly conducting the *analytical* investigation of protein and polysaccharide-based natural *biomateriomes* such as bones, cytoskeletons, and wood. Understanding the *biomateriome* could provide a blueprint for bioinspired, high-performance functional synthetic materials [1].

Combining underlaying design principles of hierarchical biocomposite structures with the rich chemistry accessible in synthetic systems may enable fabrication of composites with unprecedent properties and functionalities. This bioinspired approach requires quantification of design principles occurring in nature and their creative application to the stronger synthetic building blocks and external conditions of engineering applications [10]. Answering the challenge to create diverse multifunctional hierarchical composite superstructures that span to the nanoscale requires the emergence of novel technological paradigm. Bioinspired hierarchical ceramic composites were prepared with greatly enhanced toughness compared to their constituents using SA, brick and mortar, patterning, spinodal decomposition, and 3D printing strategies [11–18]. Nanocomposites composed of block copolymers (BCPs) and nanoparticles (NPs) have attracted much attention because BCPs organize into diverse multiphase structures [19] at various length scales with nanoscale periodicity and because of the recognition that the properties of even ordinary polymers can strongly benefit from the addition of suitable NPs. Attempts to prepare supramolecular NSBBs were made using well-defined inorganic NPs (SiO_2, laponite, graphene, CNT (carbon nanotube), etc.) and/or supramolecules (POSS (polyhedral silsesquioxane), C60, fullerene like NPs, etc.) grafted/substituted with various structure and functionality organic chains [20,21]. The synthetized amphiphiles and polyphiles provide a range of potential interactions and shapes resulting in self-assembling of nanospheres, nanocones, nanowires, micelles, vesicles, dendrites, spirals, etc. The main restriction of the bottom-up composite assembly relying solely on the SA is the low efficiency of this process and the submicron length scale associated with it. Hence, new paradigm based on external stimuli commanded assembly may be a plausible strategy to develop further the bottom-up composite fabrication nanotechnology.

It has been proposed that advanced structural composites will benefit from new features, which can be designed modifying structure on the nanoscale inspired by biological composite structures such as bones featuring hierarchical arrangement structural components based on mineralized collagen fibril as the NSBB. The analysis of mechanical properties of protein materials is an emerging field that utilizes mechanistic insight, based on structure–process–property relations in its biological context, to probe deformation and failure phenomena at the molecular and microscopic levels.

Proteins constitute critical building blocks of a diverse group of biological materials, ranging from spider silk to bone, tendon to the skin, all which play an important role in providing key functions to biological systems [22–25]. These materials are distinct from the conventional references to structure and material, as it connotes the merger of these two concepts through hierarchical formation of structural elements that range from the nanoscale to macroscale [26,27]. This merger of structure and

material is critical for biological protein materials to reach superior properties, in particular for their ability to combine disparate properties such as toughness and stiffness [28] or their intrinsic ability to adapt, change, and remodel.

The use of multiscale modeling and simulation methods has become a widely used strategy in furthering our understanding of biological protein materials. Specifically, the integration of multiscale experimental and simulation tools has led to advances in appreciating the complex change of material properties across scales and hierarchy levels [29]. In such models, the elasticity of the polypeptide chain is captured by simple harmonic or anharmonic (nonlinear) bond and angle terms, whose parameterization is informed from lower level higher fidelity models in the multiscale scheme. Such methods are computationally quite efficient and capture for example shape-dependent mechanical phenomena in large biomolecular structures, and can also be applied to collagen fibrils in connective tissue as well as mineralized composites such as bone. Results from such coarse-grained models can be used in larger level models, for example in finite element simulations as demonstrated for collagenous tissues. The evolution of protein materials through genetic selection and structural alterations has resulted in a specific set of protein building blocks that define their structure. A fundamental difference between engineered materials and naturally formed biological materials is that functionality in biology can be created by arranging universal building blocks in different patterns, rather than by inventing new types of building blocks, as in many engineered materials. The formation of hierarchical arrangements provides the structural basis to enable the existence of universality and diversity within a single material. This combination of dissimilar concepts may explain how protein materials are capable of combining disparate material properties, such as high strength and high robustness, together with multifunctionality.

The approach of utilizing universal building blocks to create diverse multifunctional hierarchical structures has been successfully applied in current macroscale engineering paradigms. For example, in the design of structures such as buildings or bridges, universal constituents (bricks, cement, steel trusses, glass) are combined to create multifunctionality (structural support, living space, thermal properties, light harvesting) at larger length scales. The challenge of utilizing similar concepts that span to the nanoscale, as exemplified in biological protein materials, through the integration of structure and material, could enable the emergence of novel technological concepts. A key obstacle in the development of new materials lies in our inability to directly control the structure formation at multiple hierarchical levels.

Up until now, the hierarchical arrangements of multi length scale structural geometries have not yet been widely utilized for most engineering applications. Many biological materials may have developed under evolutionary pressure to yield materials with multiple objectives, such as high strength and high robustness, a trait that can be achieved by utilization of hierarchical structures. The use of these concepts may enable the development of self-assembled *de novo* bioinspired nanomaterials based on analogs to peptide and protein NSBBs. Most of the recent state-of-the-art *bottom-up* formed nanostructured composites aimed at use in nonstructural applications such

as photovoltaics, optical, electrical and magnetic devices, sensing, catalysis, separation processes, and drug delivery.

In spite of their widespread commercial success, current structural fiber-reinforced composites (FRCs) exhibit number of shortcomings [29–31]. Attempts have been made to circumvent these shortcomings by employing 3D fiber architecture [32] and by making their structure hierarchical to some extent by adding nanosized fillers to the micrometer-sized reinforcing fibers [33–37]. There were attempts to develop composites with controlled 3D spatial distribution and orientation of reinforcements to answer the desired external loading requirements as well as actuation and other functions [38–42]. Further, design principles observed in nature composites were translated into fabrication of synthetic composites for a range of applications using lithography [43–45], templating [46], and other strategies replicating biomineralization [47–50]. These attempts, though very successfull, are not technologically viable to become major industrial fabrication technologies, since they are able to yield only rather small objects. Unfortunately, there is also no generally accepted model applicable to prediction of mechanical response of the hierarchical composites [51].

Alunima micro and laponite nanoplatelet-shaped filler particles were used to produce hierarechical reinforcement in polyurethane matrix [52]. Introducing 5 vol.% of laponite and 27 vol.% of alumina platelets was optimal, resulting in 7-fold increase in strength and 29-fold increase in stiffness of the hierarchical composite compared to neat polyurethane (PUR) matrix. Placing the laponite nanoplatelets in the hard segment blocks of PUR was a prerequisite allowing incorporation of large volume of alumina microplatelets. Strong bonding of the matrix polymer to the microplatelets was necessary to obtain the desired balance of toughness and stiffness. Tape casting was used to obtain well-aligned microplatelets in both thin film and bulk composites.

Recently, the use of CNTs in fabricating hierarchical FRCs for structural applications has been reviewed [53]. The additional length scale added into the CF composites by adding CNTs was expected to obviate the common shortcomings of CF composites including poor compressive properties and resistance to delamination [54]. Weak fiber–matrix interface and inherently brittle nature of polymer matrices used in CF composites were identified as the most important factors causing the above shortcomings. Use of nanoscale fibers or fillers to enhance matrix fracture resistance and strength of the fiber–matrix interface by increasing the structural hierarchy has been investigated as an alternative to traditional approaches of matrix toughening, fiber sizing, and/or employing 3D fiber architecture. The main argument in using nanoscale additives to improve CF composite performance is scalability of the processes and their economical viability in addition to gaining additional properties and functions not present in traditional CF composites.

Technologies to integrate CNTs into traditional CF composites include infusion of a CNT-modified matrix into primary CF assembly [55,56], direct growth of CNTs via CVD [57,58] or their electrophoretic deposition [59,60] on the reinforcement fabric, direct placement of CNTs between CF fiber plies [61], grafting of CNTs onto CFs [59], and use of CNT-modified sizing [62,63].

31.3 FEATURES OF NANOCOMPOSITES RELEVANT TO HIERARCHICAL COMPOSITES

Interest in the basic study of nanostructured composite materials arose out of recognition that as discrete volumes within the constituent phases approach molecular dimensions, the morphology of the constituent phases and the intrinsic properties of the structural material become dependent upon constituent size, shape, and local and global spatial packing. The understanding of the origin of the observed large property changes and effectivity of functions remains in its infancy, partly due to the nonexistence of generally accepted molecular model of polymer nanocomposites and partly by the lack of reliable experimental data [19,20]. In addition to detailed knowledge of the molecular structure of the polymer matrix, the development of a suitable theory also requires a sufficient description of NP dispersion, SA phenomena, particle–chain interactions, and effects related to the kinetics of nanocomposite preparation processes [64].

It is accepted that evidence suggests that the long-time chain dynamics may be more or as affected as the short-time dynamics in some nanocomposites. In these cases, the particles may serve to lock entanglements in or to stabilize them, especially, when the chain–particle interactions are weak. The nanoparticles can polarize the structure of the polymeric medium to which they are added, altering the molecular packing and dynamics *near* the particle, which can indirectly change the packing and dynamics *far away* from the particle. It has been shown that the spatial distribution of trapped entanglements is related to the spatial distribution of interparticle spacing shorter than the average entanglement length [65,66] and, thus, should be related to the particle size distribution and uniformity of particle dispersion. In contrary to the continuum mechanics approach, it has also been shown that the extent of stiffened chains due to interaction with nanoparticles scales with the matrix–filler interface area being inversely proportional to particle diameter for a given v_f. It is generally agreed that a key element of the overall response of the macroscopic solid made of polymer nanocomposite is associated with how and to which extent the local chain dynamics is affected by the strength and extent of interactions between chain segments and large specific surface area particles of varying surface chemistry and how this local response is "averaged" over the structurally heterogeneous nanocomposite volume into measured properties of mesoscale continuum specimens.

State-of-the-art polymer materials are often made by adding purpose-specific NPs into a polymer matrix. NPs strongly affect the ordering and relaxation dynamics of the surrounding polymeric matrix on the segment scale level, producing extensive changes of mechanical and physical properties on much larger macroscale [67]. The dispersion of NPs in a polymer matrix is known to play a critical role in nanocomposite mechanics [68,69]. In addition to preparation protocol, the state of dispersion is affected by a number of factors, including but not limited to NP shape, loading, NP–NP interactions, NP–chain interactions, and matrix chain structure. A key obstacle in advancement of nanostructured materials lies in our inability to directly control

the structure formation at multiple hierarchically arranged length scales at reasonably short assembly period. Synthesis of novel NSBBs with structurally *encoded* hierarchical assembly principles and their utilization in assembly of structurally and functionally hierarchical composites can provide the core knowledge for the desired bottom-up material design and manufacturing paradigm. External field directed SA of surface decorated precisely defined NSBBs represents means for obtaining precisely controlled spatial arrangements of functional NPs.

The understanding of the basic physical relationships between nanoscale structural variables and the macroscale properties of polymer nanocomposites remains in its infancy. The primary objective of this paragraph is to ascertain the state of the art regarding the understanding and prediction of the macroscale properties of polymers reinforced with nanometer-sized solid inclusions over a wide temperature range. We emphasize that the addition of nanoparticles with large specific surface area to polymer matrices leads to amplification of a number of rather distinct molecular processes resulting from interactions between chains and solid surfaces. This results in a "nonclassical" response of these systems to mechanical excitations when measured on the macroscale. For example, nanoparticles are expected to be particularly effective at modifying the intrinsic nanoscale dynamic heterogeneity of polymeric glass formation and, correspondingly, recent simulations indicate that both the strength of particle interaction with the polymer matrix and the particle concentration can substantially influence the dynamic fragility of polymer glass formation, a measure of the strength of the temperature dependence of the viscosity or structural relaxation time. Another basic characteristic of nanoparticles in polymer matrices is the tendency for the particles to associate into extended structures that can dominate the rheological, viscoelastic, and mechanical properties of the nanocomposite so that thermodynamic factors that effect nanoparticle dispersion can be crucially important.

The state of the dispersion of NPs in the polymeric matrix often has a large impact on the properties of polymeric materials. Unfortunately, it often has proven difficult to form uniform and stable dispersions of NPs in polymer matrices resulting in large variations in properties for systems of the same composition prepared using different techniques. Additionally, the NPs geometry such as plate or sheetlike particles, nanotubes, or polyhedral nanoparticles can also have a large impact on property changes, since it can affect both surface energetics and surface to volume ratio. The possible underlying mechanisms for nanoparticle clustering were investigated, considering the roles played by phase separation, as well as SA that may occur before, or *in lieu* of phase separation. In addition, the way, in which the state of NPs clustering and the NPs shape both affect material properties important for applications and processing, was discussed [70,71].

There has been considerable interest in utilizing particle SA as a "bottom-up" route to new material assembly. Such particle SA is of interest because it might, for example, allow us to construct improved polymer nanocomposites with "dialed-in" properties. Specifically, the ability to assemble particles into desired morphologies should allow us to dramatically increase the electrical conductivity of typically insulating polymers. Similarly, this ability to control particle SA might permit us to synthesize a range of bioinspired materials. As an illustrative example, we point to biomimetic

systems where spherical nanoparticles of hydroxyapatite (HA) are used to create tooth enamel and bone mimics. In the former case, it is conjectured that the HA particles are organized by the biological systems into "lines." These "lines" are then stabilized by a matrix, which subsequently hardens and "freezes" in this organization. In contrast, bone has a uniform dispersion of HA particles in the matrix. Our unique ability to control nanoparticle organization might thus allow us to build such bioinspired systems for an entirely new range of synthetic applications. It has also been shown that structural proteins such as collagen can undergo SA process resembling first-order thermodynamic transitions in forming microfibrils which controls to a great extent the mineralization process to form basic building blocks of bones.

Important structural characteristics of the nanoscale reinforcement include more detailed description of the chemical texture of the surface, information regarding the local curvature of the particles in relation to the chain stiffness, and their specific surface area. Latest theoretical modeling suggests that the spatial and time distributions of interparticle distances in real nanocomposite systems with randomly packed particles are of crucial importance for the experimentally observed enormous chain stiffening [72]. For spherical reinforcement, more detail regarding the radial size distribution is important for refined predictive model development. Thus, more appropriate descriptors of the specific surface area, distribution of surface curvature, and radial distribution of the filler particles are important, since the scale of the response is correlated to the scale of the local perturbation caused by the nanoparticles. Similarly, for anisotropic particles, more detailed descriptors are necessary including information about spatial and time distribution of particle orientation. It was also agreed that multiscale descriptions and characterizations at a range of length scales are still needed so that each can be modeled with appropriate governing physics. On a contrary note, it was generally acknowledged that the stiffness and strength of the reinforcing nanoparticles is secondary when considering the bulk mechanical, rheological, and physical properties of this class of nanocomposites. More critical characteristics are associated with the polymer behavior in the interphase region which prevails over the bulk at very low nanoparticle content even in the case of spherical particles [69]. Needless to point out that the traditional meaning of the interphase as a continuum layer existing between the particle surface and some distance in the polymer bulk becomes no longer valid at the nanoscale. Experiments as well as theoretical simulations suggest that the "thickness of interphase" does not scale with particle size, as often proposed [73]. In a simple case of regular cubic lattice of monodisperse spheres, the average interparticle distance reaches particle diameter D for about 7 vol.% of the filler, while for random packing of the same spheres, this limit is reached at 2.6 vol.% of the filler. For spherical particles with $D = 10$ nm and common amorphous polymer with radius of gyration R_g equal to about 5 nm, at this volume content, all the chains are in contact with particle surface and there is no bulk polymer. Moreover, interphase layer is usually described as a layer with properties distinct from both filler and the polymer bulk or with a property gradient. Such a description is no longer valid at the length scale of a single macromolecule and becomes even more complicated in the case of entangled chains.

31.3.1 INTERFACE/INTERPHASE AT NANO- AND MICRO LENGTH SCALE

In FRCs, exhibiting heterogeneous structure at multiple length scales, the interphase phenomena at various length scales were shown to be of pivotal importance for the control of the performance and reliability of such structures [68]. Various models based on continuum mechanics were used to describe effects of the macro- and mesoscale interphase on the mechanical response of laminates and large FRC parts, satisfactorily. At the microscale, the interphase is considered a 3D continuum with ascribed average properties. Number of continuum mechanics models was derived over the last 50 years to describe the stress transfer between matrix and individual fiber with realtively good success. In these models, the interphase was characterized by some average shear strength, τ_a, and elastic modulus, E_a. On the other hand, models for transforming the properties of the microscale interphase around individual fiber into the mechanical response of macroscopic multifiber composite have not been generally successful. The anisotropy of these composite structures is the main reason causing the failure of these models. The strong thickness dependence of the elastic modulus of the microscale interphase suggested presence of its underlying substructure.

On the nanoscale, the discrete molecular structure of the polymer has to be considered. The term interphase, originally introduced for continuum matter, has to be redefined to include the discrete nature of the matter at this length scale. The segmental immobilization resulting in retarded reptation of chains caused by interactions with solid surface seems to be the primary phenomenon which can be used to redefine term interphase on the nanoscale. Thus, the reptation model and a simple percolation model were used to describe immobilization of chains near solid nanoparticles and to explain the peculiarities in the viscoleastic response of nanoscale "interphase." It has also been shown that below 5 nm, Bernoulli–Euler continuum elasticity becomes not valid and higher order elasticity along with the proposed reptation dynamics approach can provide suitable means for bridging the gap in modeling the transition between the mechanics of continuum matter at the microscale and mechanics of discrete matter at the nanoscale.

The role of the nanoscale "interphase" to control the performance and reliability of the FRC parts has to be considered from two perspectives: (i) low v_f nanocomposites ($v_f < 0.05$) and (ii) high v_f nanocomposites ($v_f > 0.85$). The (i) represents the direction to preparing new nanostructured advanced matrices while the (ii) leads to designing new nanostructured advanced reinforcements. With few exceptions, most of the published literature on the synthetic nanocomposites deals with the low v_f nanocomposites, while, on the other hand, most of the literature published on high v_f nanocomposites is related to the mechanics of biocomposites such as bones, teeth, and shells.

Most of the experimental evidence related to the interphase in the low v_f nanocomposites were obtained at temperatures below the polymer T_g using mesoscale test specimens. Assuming the chain immobilization to be the primary reinforcing

mechanism on the nanoscale, spatial distribution of the conformation entropy within the polymer phase is of primary importance. Hence, experimental data for nanocomposites above the matrix T_g has to be considered. Sternstein and Zhu [73] published interpretation of the viscoelastic response of rubbery nanocomposite above the matrix T_g, i.e., the Payne effect. Kalfus and Jancar [74–76] analyzed the viscoelastic response of polyvinylacetate filled with nanosized HA over the temperature range from −40°C to +120°C and observed strain softening similar to the Payne effect. The modulus recovery experiments allowed to determine the terminal relaxation time of reptation motion of bulk and surface immobilized chains, supporting the hypothesis that there is no "interphase" per se when nanoscale is considered. In order to bridge the gap between the continuum interphase on the microscale and the discrete molecular structure of the matrix consisting of freely reptating chains in the bulk and retarded reptating chains in contact with the inclusions, higher order elasticity combined with a suitable molecular dynamics model could be utilized.

It was demonstrated that the large specific surface area of the nanosized filler is capable of immobilizing large amount of entanglements causing the steep increase of E' with small addition of nanoparticles [77]. This observation seemed to confirm the purely entropic character of the reinforcement mechanism on the nanoscale. All the data published support the dominant role of the chain immobilization as the main reinforcing mechanism.

In the light of the existing experimental evidence, it seems that the term "interphase" defined as a continuum phase of limited extent loses its physical meaning when considering true nanocomposites. Due to 2 orders of magnitude greater specific surface area of the true nanofillers, almost all the polymer chains are in contact [75] with the surface at very low filler loadings above 2 vol.%. In addition, continuum mechanics has only limited validity at this length scale and the discrete molecular structure prevails resulting in strong effect of nonlocal character of viscoelastic response of the nanocomposite matrix.

The interphases in high v_f nanocomposites were studied using the abalone shells [78]. These shells represent a laminated sheet-reinforced composite with over 95 vol.% of aligned 500 nm thin aragonite sheets embedded in a protein matrix in apparently mesh-like fibrillar form. In the work of Hansma et al. [79,80], the model of sacrificial bonds has been proposed to explain the observed high fracture resistance of nacreous composites. It has been shown that the hypothesis of the sacrificial bonds can also be used to simulate deformation response of lightly cross-linked long flexible chain network polymer fibril. In order to apply the model to the behavior of an ensemble of chains in the vicinity of rigid weakly attractive nanometer-sized inclusion, the immobilization phenomenon has to be investigated as the source of the drastic change in the viscoelastic behavior of polymers with addition of small amount of nanoscale inclusions.

Reducing the size of rigid inclusions from micro- to nanoscale is accompanied by 2–3 orders of magnitude increase in the internal contact area between the chains and the inclusions. Moreover, above 2 vol.% nanoparticle content, the average interparticle distance is reduced below radius of gyration, R_g, of the chains. Hence, the chains

in contact with the solid surface possess reduced segmental mobility at temperatures $T \geq T_g$. Below T_g, main chain segmental mobility is frozen and only secondary low temperature side chain mobility can be affected. In addition, the conformation statistics of chains near solid surface can be altered from Gaussian random coil to Langevin coil above T_g and this phenomenon can be transformed into the behavior of immobilized chains also upon solidification below T_g.

In order to characterize the reduction in chain mobility in an entangled melt quantitatively, one can use the characteristic reptation relaxation time, τ_{rep}, introduced by deGennes [81]. The τ_{rep} is given for an entangled chain as

$$\tau_{rep} \cong \frac{L^2}{D_c} \cong \frac{NL^2}{D_0} \tag{31.1}$$

where L is length of the reptation path, N is number of monomer units in a chain, D_c and D_0 are diffusion constants of a chain and a monomer, respectively. The terminal relaxation time of a chain in a neat polymer melt can be expressed in a number of ways. Lin has expressed the τ_{rep}, taking chain contour length fluctuation into account, in the form:

$$\tau_{rep} = \frac{L_0^2}{\pi^2 D_c} \cong \frac{b^2 \zeta_0 N^2}{\pi^2 k_B T}\left(\frac{M}{M_e}\right)\left[1 - \left(\frac{M_e}{M}\right)^{1/2}\right] \tag{31.2}$$

where ζ_0 is monomer friction coefficient, b is length of the statistical segment, k_B is the Boltzmann constant, T is absolute temperature, and M_e is number of monomer units per one entanglement strand.

In the case of a chain interacting with a filler surface and entangled with neighboring chains, the question of primary importance is how to establish a connection between the static conformation structure and the chain dynamics. In spite of certain intramolecular order, the chain in a melt can be considered a random Gaussian coil. If such a chain approaches a solid surface, its conformation transfers to the train-loop-tail structure and the chain conformational entropy as well as the chain internal energy can alter very substantially depending on the surface–polymer interaction energy, e_{fp}, under given conditions. Assuming the chain friction coefficient, ζ_c, in the form:

$$\zeta_c = \zeta_0 N + \zeta_a N^{1/2} \tag{31.3}$$

where ζ_a is the friction coefficient of an adsorbed monomer unit and the number of monomer units in trains is $N_a = N^{1/2}$ for the weakly interacting surface, the terminal relaxation time is in the form:

$$\tau_{rep}^{ads} = \frac{L^2}{2D_c} = \frac{b^2 N^{5/2}}{2k_B T N_e}[\zeta_0 N^{1/2} + \zeta_a] \tag{31.4}$$

Kalfus and Jancar [75] extended the use the above Rubinstein model [82] to describe the reptation time of a linear chain weakly interacting with nanofiller surface.

Friction coefficient, ζ_a, is very difficult to measure and it is known just for the system silica-polystyrene at 153°C. Estimation of the ζ_a was based on the theoretical analysis given by Lin [83]. Thus, one can establish a relation for the reptation time of a surface adsorbed chain as follows:

$$\tau_{rep}^{ads} = \frac{b^2 N^2}{\pi^2 k_B T N_e}[\zeta_0(N - N_a) + \zeta_a N_a] \tag{31.6}$$

In the case that $N_a = N^{1/2}$, the reptation time takes the form:

$$\tau_{rep}^{ads} = \frac{b^2 N^{5/2}}{2\pi^2 k_B T N_e}[\zeta_0 N^{1/2} + \zeta_a] \tag{31.7}$$

To describe the change in reptation dynamics of the chains as a function of nanoparticle volume fraction, percolation model was used [75]. At the percolation threshold, physical network formed by interconnection of immobilized chains on individual nanoparticles penetrates the entire sample volume. In this case, only physical "cross-links" are considered and the terminal relaxation time reaches the value characteristic for the lifetime of the physical filler–polymer bond. Thus, the relaxation time near the percolation threshold is expressed in the form [75]:

$$\tau_{composite}^{rec} = \tau_{rep}^{ads} v_{eff} \left(\frac{v_{eff} - v_{eff}^*}{1 - v_{eff}^*} \right)^b \tag{31.8}$$

where v_{eff}^* is critical effective filler volume fraction ($v_{eff}^* = 0.04$ for PVAc-HAP at 90°C) and b is the percolation exponent ($b = 4$ for the same system). The v_{eff}^* is a sum of the filler volume fraction and the volume fraction of immobilized chains and was equal to 0.04 for PVAc-HAP nanocomposites at 90°C. To simplify the percolation, random clustering of effective hard spheres was considered only in the way similar to that originally outlined by Jancar et al. [84] for microscale composites. Percolation threshold at approximately $2\,m^2$ of the filler–polymer contact area per 1 g of the composite was found in PVAc-HA nanocomposite system. All the chains were immobilized at the internal contact area of $42\,m^2$ per 1 g of the nanocomposite.

31.3.2 REINFORCING MECHANISMS AT MULTIPLE LENGTH SCALES

The reinforcing mechanism in particle-filled polymers consists of three main contributions. The first one, related to replacing portion of low stiffness polymer with more rigid particles, is size independent. The second one consisting of stress transfer into nonspherical particles due to shear stress developed at the particle–matrix interface,

and the third related to chain stiffening due to dynamical and packing restriction at the segment scale are strongly related to the particle size. Contribution from particle–particle interactions has also been proposed to explain viscoelastic behavior of rubbers [85] and deformation response of polymer nanocomposites [86]. At low temperatures or short times, the low conformational entropy state of matrix chains leads to the phenomenon that amorphous nanocomposite behaves as two-phase particle-polymer system with reinforcement, which is in good agreement with micromechanics models [87]. Thus, in nanofilled glass polymers the reinforcement is primarily given by the mechanical contributions. Molecular stiffening contribution becomes pivotal importance at longer times or higher temperatures. No generally accepted model exists to predict this effect in a satisfactory manner.

Recently, attempts have been made to understand molecular mechanisms leading to significant increase of elastic modulus with the nanofiller content above T_g of matrix. A very general approach has been proposed by Riggleman et al. [88] attributing the observed steep increase in elastic modulus to alternation of the spatial distribution of chain relaxation times and changes in the chain packing near attractive or repulsive particles. In a more practical model, Zhu and Sternstein [89] have introduced the model of trapped entanglements to describe the steep increase of elastic moduli of PVAc with the content of silica nanoparticles and to explain the Payne effect in rubbery nanocomposites. The Riggleman model assumes implicitly the random distribution of the antiplasticizer molecules, however, the spacing between them is not explicitly described. On the other hand, Sternstein model considered effect of interparticle spacing, however, only in the simple case of cubic particle packing.

It was found that for random packing, a significant portion of interparticle distances is shorter compared to the cubic packing and, at the same time, shorter than the chain length necessary to form entanglements. Thus, in the framework of the Sternstein model, the random particle packing is an essential for enhancing chain incremental stiffness due to strong chain confinement via interaction with filler surfaces at much smaller filler content than predicted using uniform particle spacing.

In order to understand and predict mechanical behavior of polymer nanocomposites, the proposed models have to be able to relate highly localized nanoscale structural information to the behavior observed on the mesoscale. Such models are based on an assumption that the mechanical response of the system can be considered localized and that the system is ergodic, thus, the common homogenization procedures are applicable. This approach has been highly successful for predicting behavior of crystals and slightly less successful in predicting behavior of polycrystals. As shown by Maranganti and Sharma [90], polymers represent systems with highly nonlocal deformation behavior and, thus, traditional continuum mechanics cannot be used and higher order elasticity combined with molecular dynamics has been suggested as a reasonable framework to be used with amorphous solids. In addition, reducing the scale at which the structural information is considered below the critical representative volume element (RVE), the averaging of stresses and strains is no longer ergodic. This is even more complicated by the presence of heterogeneities such as rigid nanoparticles causing drastic changes in dynamics and packing of

chains in their vicinity, and also chains further from their surface. As a result, structure–mechanical response relationships for a polymer nanocomposite in the glassy state cannot be completely understood without understanding effects occurring in the liquid state and during the solidification transition.

Macroscopic relaxation processes occurring on a molecular level play decisive role in macroscopically measured viscoelastic manifestations of amorphous polymers. These molecular processes include, in hierarchical order, local vibration motion of monomer units, cooperative conformation transitions, and normal mode motions. Single bond cooperative conformation transitions are of pivotal importance for the homogenization of the chain conformation structure and, hence, for the onset of the glass transition. It has been shown by Boyd and Smith [91] that these conformation transitions are mostly realized in form of sequences with various transition rates. Thus, one of the manifestations of local conformation dynamics is that bond sequences in form of waves of conformational transformation diffuse along a chain with rate depending on local packing effects.

As soon as the chain is conformationally ergodic, normal mode oscillations start to be responsible for the fluctuation of the chain end-to-end vector. This relaxation mechanism is significantly dependent on the length of chains considered. Hence, after the initial drop of time-dependent elastic moduli, $G(t)$, within the mechanical glass transition region $G(t)$ adopts slope predicted by the Rouse model [92], $G(t) \propto t^{-1/2}$. It means that longer and longer "standing waves" of Rouse segments are involved in the relaxation process as time evolves. In long chain melts, this relaxation process is disturbed by topological constraint of entangled polymer chains. Enormous interpenetration of chains and its uncrossability leads to the phenomenon that chains can move by slipping over each other and not slipping through each other. Due to this constraint, certain effective chain lengths are responsible for appearance of entropy-driven elastic resistance persisting over time scale given primarily by the chain molecular weight. On very long-time scale, polymer chains move as if they were phantom—time dependence of the mean square center of mass displacement is scaled as $g_3 \propto t^1$. This frame seems to be crucial for addressing the true mechanisms leading to the observed viscoelastic behavior of polymer nanocomposites because nanoparticles are able to alter drastically chain diffusive motion due to extensive filler–polymer interface area and causing local geometrical constraint with range comparable with chain dimensions.

Sternstein et al. [73,89] assumed that the average interparticle distance is comparable with the chain end-to-end distance even at low filler volume fractions, v_f. Adsorption of chains onto nanoparticle surface leads to the creation of surface-chain loops and interparticle bridges. These chain segments can be relatively short and their conformation statistics deviates from the Gaussian behavior significantly. Elasticity of non-Gaussian chains can be described using the Langevin function-based theory of rubber elasticity. Moreover, these short chain segments are in a state that is more elongated than the chain end-to-end distance referred to as the reference state bias. Under given time scale of measurement, average lifetime of filler–polymer bonds is long enough so that the non-Gaussian chain segments can

behave in a way similar to chains between junctions in a chemical network. Such a system exhibits substantially greater stiffness compared to a long Gaussian chain network. From the arguments put forward above, the importance of the interparticle spacing becomes obvious.

Sternstein's theory of nanocomposite reinforcement is based on the Langevin rubber elasticity of finite chain segments situated at the filler–polymer interface. This theory considers elasticity, which takes only changes of conformation entropy upon chain loading into account. As the chain extension approaches its limit, corresponding to *r/Nb*, the conformation entropy of a chain segment drops and the chain retractive force increases very rapidly. The retractive force can be then expressed as

$$f = \frac{k_B T}{b} L^{*}(r/Nb) \tag{31.9}$$

where k_B is the Boltzmann constant, T is temperature, L^* is the inverse Langevin function, r is the chain end-to-end separation, N is number of monomer units, and b is the monomer unit length. The elasticity of short chain segments has to take into account the bond angle, which is under given conditions almost undeformable. This leads to the correction of the full extension of the vinyl-type chains (like PE, PS or PVC) by a factor of 0.816 resulting in the maximum length of fully extended chain being equal to $0.816Nb$ instead of just Nb as in the case of freely jointed chain [93]. The retractive force, expressed by the Langevin function, is substantially greater than that obtained using Gaussian statistics for chains of finite size.

Even though the proposed model does not require a precise definition of the chain entanglement, it seems worth to provide rather broad definition of this term. In no instance, the chain entanglement considered here is simply a nod formed by two "shoe string" chains as often described in the literature. Regardless of the true meaning of the term entanglement, it is obvious from numerous relaxation experiments that certain characteristic internal distance is typical for behavior of high molecular weight polymers above T_g. Such a distance represents some kind of constraint range for normal mode fluctuations of chain segments and can be approximated by a tube of diameter, d_T. However, the space d_T^3 is not occupied by one entanglement strand only, the cubed tube diameter involves approximately 15 other chain strands. Thus, for the purpose of the proposed model, the entanglement is considered a cooperatively moving group of chain segments changing in time and space. The interparticle spacing represents a constraint to the chain mobility principally very similar to the tube due to surrounding chains in neat polymer. Chain confined between nanoparticles must reptate over the constraining surfaces during its relaxation. This process needs more energy in the presence of nanoparticles compared to the neat polymer. Thus, as v_f increases, the effect of trapped entanglements increases at the expense of chain entanglements. Experimentally, one can observe rubbery plateau even in nanofilled short chain melts and very long persisting rubbery plateau in long chain melts, where complete elasticity drop is beyond laboratory time scale.

31.3.3 EFFECT OF PARTICLE DISPERSION

The state of agglomeration could be described by a pair correlation function [94] $G(d)$:

$$G(d) = \frac{V}{N^2}\left(\sum_n \sum_{n \neq m} \delta\left(d - \left|\mathbf{x}_m - \mathbf{x}_n\right|\right)\right) \tag{31.10}$$

where N is the number of particles in the examination volume V, $\mathbf{x}_m$ and $\mathbf{x}_n$ denote the position vectors of the particles m and n, respectively, and δ is the Dirac delta function. It sums the probability for particles to be located in a certain center-to-center distance d, therefore regular structures result in peaks in $G(d)$ but it is not a correlation function in term of statistics [95].

Colloidal chemistry provides the well-established DVLO theory to describe the agglomeration-dispersion phenomena [96]. Colloidal particles agglomerate due to the van der Waals attraction if the Coulomb repulsion, which depends on the ionic strength of the suspension and on the surface charge, as quantified by zeta potential ζ, is not sufficiently strong to keep them dispersed. For sufficiently strong Coulomb repulsion, a primary energy minimum with an energy barrier exists which leads to kinetically controlled agglomeration. For an intermediate ionic strength and a high or intermediate zeta potential, the shallower secondary minimum becomes deeper than $2\ k_B T$ and entraps particles in less stable secondary agglomerates, which stability is more sensitive to particle size than of the primary agglomerates.

In polymer nanocomposites, polymer scaffolds can serve three purposes: assembling nanoparticles into clusters, inducing ordering and anisotropic orientation, or acting as a functional element. Hooper and Schweizer [97,98] performed a computational PRISM study on hard spherical particles dissolved in an adsorbing homopolymer melt and predicted four categories of polymer-mediated nanoparticle organization: contact aggregation, steric stabilization, bridging formed by adsorption of more particles on a single chain, and "telebridging" where distinct adsorbed layers coexist with longer range bridging. All types of organization are schematically visualized in Figure 31.1.

Hooper and Schweizer found the interfacial polymer–particle strength at contact and spatial range of particles attraction to play a key role in determining the state of dispersion. A miscibility window for moderate polymer–particle interaction with two types of phase separation was pronounced. The contact aggregation is favored for low affinity between particles and polymer whereas bridging prevails in case of strong attraction. These results were experimentally confirmed by Anderson and Zukoski [99]. Moreover they reported a gelation for moderate particle interaction strength at higher filler loadings and concluded that the polymer adsorption in the bridged state is reversible and thus the polymer chains can change their configuration on the surface upon cooling.

Although Hooper and Schweizer predicted a closing and an eventual disappearance of the miscibility window with increasing chain length due to the loss in the

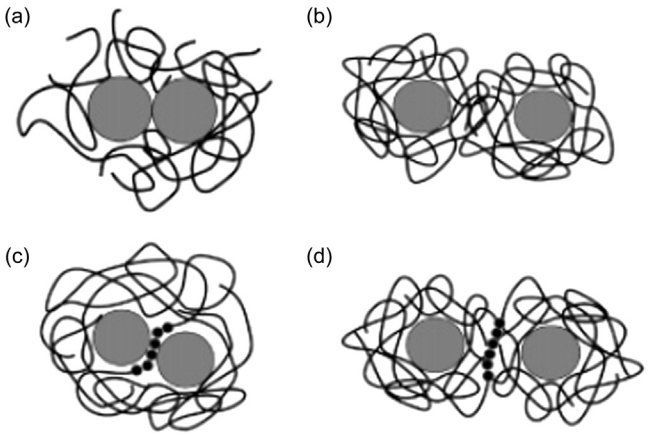

FIGURE 31.1

Schematic visualization of predicted nanoparticle organization modes: (a) direct contact agglomeration, (b) dispersion, (c) bridging, and (d) telebridging [97].

polymer translational entropy, Anderson and Zukoski observed no evidence for such phenomenon. On the contrary, Patra and Singh [12] reported conservation of the dispersion state independent on particle–chain relative size, a suppression of the direct contact agglomeration for particles bigger than the polymer radius of gyration R_g and decreasing tendency in clustering with increasing chain length for particles smaller than R_g characterized by a sequential shift from string-like to branched and spherical clusters and a cluster dissolution based on their molecular dynamics simulation. The latter effect is obviously caused by polymer-induced repulsion forces which first lead to a loss in the particle–particle site preference and eventually completely inhibit the clustering.

According to the simulation, the phase behavior exhibits an entropy-driven lower critical solution temperature type of phase separation and an enthalpy-driven upper critical solution temperature type of phase separation with a miscibility window in-between. Experimental results with three different states of organization were indeed reported by Stenhar et al. [11]. The dispersed state exhibits the highest entropy, followed by the direct contact agglomeration state and the bridged state where both the particle configuration and the polymer confinement between particles contribute to the loss in entropy. The overall potential energy of nanocomposite is dominated by polymer–particle interaction energy and decreases with increasing interaction strength. Rahedi et al. [100] modeled a clustering of nanoparticles in polymer melt with strong short-ranged attractive and weak long-ranged repulsive forces and concluded that such system exhibits a SA transition temperature at which most of the clusters from the low temperature highly clustered state extinguish and a high temperature highly dispersed state is formed; however, the clusters are partially preserved at higher filler loadings.

To comment on solvation effects, an appropriate physicochemical measure of solvent capabilities is indispensable. Compatibility between polymers and solvents is often described by Hansen's total solubility parameter δ. The solubility parameter is defined as the square root of the cohesive energy density [101]:

$$\delta = \sqrt{\frac{\Delta E_{\text{vap.}}}{V_{\text{m}}}} \tag{31.11}$$

where $\Delta E_{\nu\text{ap}}$ is molar energy of vaporization and V_{m} denotes molar volume of the liquid. Substances with a $\Delta\delta < 7\,\text{MPa}^{0.5}$ are likely to be miscible, whereas immiscibility is probable with $\Delta\delta > 10\,\text{MPa}^{0.5}$. Hansen separated this one-dimensional parameter into three types of partial solubility which originate from dispersion δ_{d}, polar δ_{p}, and hydrogen bond δ_{h} contribution:

$$\delta^2 = \delta_{\text{d}}^2 + \delta_{\text{p}}^2 + \delta_{\text{h}}^2 \tag{31.12}$$

In solution, the nanoparticle affinity to polymer must exceed the nanoparticle affinity to solvent for an assembly to occur. Dissolution of nanocomposite induces a dilution of polymer segments and a reduction in repulsive interactions between particles; however, Kim and Zukoski [102] reported that miscibility is not directly tied to solvent quality. At laboratory temperature, particles of a PEG-silica nanocomposite experienced higher repulsive forces in water (good solvent conditions) than in ethanol (near theta-solvent conditions) but at elevated temperature, water (near theta-solvent conditions) segregated to the surface and polymer to the bulk due to the reduced particle repulsion whereas no change appeared in the ethanol (good solvent conditions) solution.

Kalra et al. [103] investigated an influence of shear on nanoparticle dispersion in polymer melts by a coarse-grained molecular dynamics study. They concluded that shear significantly affects the aggregation kinetics, whereas the equilibrium state of dispersion remains unchanged. They claimed that shear induces rupture-like deformation and causes a nonmonotonic dependence of diffusivity on shear rate with a critical point at which the decreasing diffusivity turns into increasing with increasing shear rate. The minimum in diffusivity is suppressed for short chains but deepens and shifts to higher shear rates with increasing degree of polymerization. The diffusion constant of small colloid particles with radius smaller than the polymer radius of gyration exceeded the prediction of the Stokes–Einstein equation and exhibited no dependence on polymer molecular weight.

Since nanoparticles are often dispersed in a matrix in thermodynamically nonequilibrium state, a kinetic insight on aggregation phenomena would be more relevant to practical applications; however, only little is known and further research in this field is necessary. Smaller particles experience faster diffusion and therefore also faster aggregation, on the other hand the aggregation rate becomes very slow below the glass transition temperature [104]. The potential of mean force (PMF) exhibits a

higher oscillation tendency and more energy wells separated by energy barriers with increasing polymer–particle interaction strength thus leading to an assumption that a formation of kinetic structures dominates the behavior of such systems. This is in agreement with the statement of Stenhar et al. [11] who claim that ionic interactions frequently lead to extended networks arising from kinetic entrapment.

While NP dispersion is believed to critically affect properties, it is not apparent that a single state of particle dispersion or organization should optimize any given macroscale properties. It was suggested [95,105,106] that there exist cross-property bounds between different transport properties of a macroscale composite. Using these bounds allows us to predict the secondary phase dispersion state that optimizes one or multiple properties of the composite. This immediately suggests that optimizing one versus two properties of a composite can require very different morphologies. While this idea is new and unproven in the field of PNCs, it suggests that the creation of multifunctional composites requires exquisite control over NP spatial distribution [107–109]. Making such connections between NP dispersion and organization with macroscale properties is then a crucial aspect that is only now beginning to be considered [35–38]. Since polymer chains and NPs are similar in size, competition may exist between NP and chain SA in the liquid phase affecting the evolution of the NPs spatial distribution upon solidification. In amorphous polymers, the supramolecular structure established in the transition from equilibrium liquid to nonequilibrium glass is kinetically controlled. Hence, the preparation protocol is of paramount importance for the state of NP dispersion and PNC properties.

To simultaneously optimize more than one property of the composite superstructure requires that the constituent "phases" are connected in a multiply periodic fashion [95]. This immediately suggests that optimizing one versus two properties of a composite can require very different morphologies. Understanding must be achieved of the fundamental links between NSBB syntheses, hierarchical structure SA, properties and functions at multiple length *and* time scales requiring interdisciplinary approach integrating concepts and techniques from engineering, material science, structural biology, chemistry, and physics. Possible algorithms capable of capturing physically sound averaging procedures transforming the mechanical response of the variety of local nanoscale structures discrete in nature into the global response of macroscale continuum have not been discovered yet. Revealing the connections between NSBB dispersion and organization with macroscale properties is a crucial aspect that will be quantified by developing suitable interdisciplinary theoretical framework. The development of such a new framework requires the design and execution of specifically designed experiments to provide simultaneously reliable structure and property data over many length and time scales not present in the current literature. We believe that the discovery of the basic natural laws governing the SA of NSBBs in the polymer matrix is crucially important in developing responsive hierarchical polymer materials and technologies for their manufacturing.

The dispersion of NPs in a polymer matrix is known to play a critical role in nanocomposite mechanics. In addition to preparation protocol, the state of dispersion is affected by a number of factors, including but not limited to NP shape, loading,

NP–NP interactions, NP–chain interactions, matrix molecular structure, temperature, and external force fields. The state of NP assembly/dispersion in the polymer matrix is affected by its chain molecular weight, regularity and stiffness, NP shape and loading, NP–NP and NP–chain interactions the most [97,98]. The NP assemblies in a polymer can take the form of *agglomerate, cluster, or a uniform distribution* of individual NPs with random or regular spatial organization [98], resulting from a complicated interplay between enthalpy (agglomeration) and entropy (dispersion) in the liquid phase, the preparation protocol and kinetics of solidification. However, the possible underlying mechanisms for the NP spatial organization have not been discovered, yet, and the kinetics of these processes remains a significant challenge for polymer physics. In order to obtain basic laws governing the multi length and time scale structure–property–function relationships in hierarchical composites, well-controlled NP dispersion must be obtained. Discovering thermodynamic and kinetic parameters controlling SA of surface decorated, precisely defined NPs and relating them to the NSBB synthesis is fundamental for developing advanced technologies capable of fabricating large hierarchical composite superstructures. Understanding mechanisms and kinetics of SA of surface decorated precisely defined NPs represents means for obtaining precisely controlled spatial arrangements of NPs [110] under technologically viable conditions. No theoretical framework has been published describing the laws governing multi length scale assembly of NSBBs or NPs into hierarchical superstructures.

It is a great challenge to fully understand dispersion and clustering of NPs in the PNCs through experimental techniques. Thus, equilibrium coarse-grained MD simulations of NP assembly in polymer melt/soulution were performed [111]. Hooper and Schweizer proposed four types of soft repulsion particle–particle potential field resulting in NP aggregation, bridging, steric stabilization, and telebridging. Increasing the NP volume fraction (v_f) induced transition from highly bridged or sterically stabilized clusters to more diffuse liquid-like packing characterized by many body clustering. The model predicts that agglomerates form at weak interfacial attractions, uniform dispersion occurs at intermediate chain–NP attraction and clustering is observed for strong interfacial attraction [112]. It was also shown that there are two types of clustering transitions, one due to thermodynamic response and the other due to dynamical response [113]. According to our knowledge, none of the results published so far reported on the morphology evolution during transition from equilibrium melt to the nonequilibrium glassy state, even though, most of the experimental observations were made using solid specimens [12,110]. In the case of modeling microparticle clustering in polymers with negligible amount of chains in contact with particle surface, the equilibrium models describe the structure and properties satisfactorily. The specific interface surface area (S_f) is indirectly proportional to the particle diameter, hence, as already shown, nonequilibrium state to which polymer vitrifies is not affected by microparticles significantly and remains the same as for the neat polymer. In PNCs, however, the large S_f alters packing and dynamics of a substantial portion of the chains, thus, the system is arriving at significantly different nonequilibrium state compared to the neat matrix vitrified under the same conditions

making the use of results of equlibrium MD simulations for interpreting behavior of supercooled nonergodic PNCs questionable.

The geometry of NP assemblies formed under the thermodynamic equilibrium is related to the single NP shape and surface energetics [110]. Inorganic NPs are typically immiscible with an organic phase resulting in a competition between NP SA and phase separation. To date, there have been several successful demonstrations of techniques that induce liquid state SA of NPs resulting in structures resembling chains and wires, hexagonally arranged particles, worm-like and labyrinth-like structures, precise clusters, nanowires, and onion-like vesicles, as well as aggregates with little or no order. Similarly, flow effects can also be used to assemble particles into anisotropic structures. At the same time, shear flow significantly slows down formation of NP rich domains and affect their structure [103].

Understanding how structure at nano- and microscales affects the mechanics and functions of hierarchical composites at macroscale is still in its infancy [67]. NPs alter the segmental packing near their surface and heterogeneity of spatial distribution of segmental mobility [114]. In an equilibrium melt, the NP–segment interaction energy affects the mobility at a distance up to three segment lengths from the surface. For weak attractive interactions, NPs in the clusters form a network separated by polymer chains with a possibility for adsorption-induced vitrification of chains inside the clusters [99,115]. The NP-induced segmental orientation and limited extensibility of chain bridges may greatly contribute to the nonclassical reinforcement observed in polymer nanocomposites [116]. Rigglemen et al. [117] showed that NPs can act as entanglement attractors, and thus trapping the chain's primitive path at large deformations. The capacity of the clustered NPs to percolate the polymer bulk may greatly affect the large strain deformation behavior of these hierarchical superstructures.

The existence of thermodynamically phase-separated states is ubiquitous in mixtures. NP clustering via phase separation is particularly common if there are unfavorable polymer–NP interactions, relative to the NP–NP interactions. Indeed, when polymer–NP interactions are highly unfavorable, there may be no thermodynamically stable NP dispersion. Here, we focus on situations where a stable dispersion is possible, and examine the NP clustering process. The state of dispersion is affected by a number of factors, including particle loading, interparticle interactions, and temperature. We have found that the specific heat can be a reliable metric to determine the state of dispersion, since specific heat is sensitive to energy fluctuations related to particle dispersion. Specifically, when particles are in a stable dispersion or clustered state, there are little fluctuations in energy, since the "phases" are highly stable. However, between the limiting assembled and dispersed states, particles can aggregate into small, short-lived clusters, resulting in large fluctuations energy, and hence large specific heat. To illustrate this, we plot specific heat as a function of temperature for several loading fractions and find a pronounced maximum at intermediate loading. The peak in specific heat defines the crossover between dispersed and assembled states, and the energy determines that the assembled state occurs at low temperature (also identifiable by visual inspection). If dispersion was to be analogous to the phase separation of a binary

mixture, we would expect that u_{pp} and c_{pp} would exhibit a discontinuity, provided we do not follow a path through the critical point. Additionally, if the transition was first order, we would expect hysteresis in the vicinity of the transition. In a narrow region near the transition, our results would depend on which direction we approach the transition. This possibility was tested, and they found no evidence of hysteresis. These results suggest the transition is not first order [14].

If the crossover between clustered and dispersed states is not a simple phase transition, how can we characterize it? We use the specific heat data to calculate the "clustering diagram." Specifically, for each, we define the approximate boundary temperature, T^*, between clustered and dispersed states by the location or the peak of specific heat, c_{pp}. The boundary is positively sloped, indicating that clustering occurs for large v_f and low T. Comparing the behavior of the amplitude and location of the maximum of c_{pp} provides us with further evidence against phase separation via a first-order transition. The decrease in the amplitude of the c_{pp} peak with increasing v_f is consistent with the predicted behavior for an associating system [14]. The model of equilibrium polymerization specifically predicts that the loci of specific heat maxima should shift location according to:

$$v_f^{crit} \approx exp(-E/kT^*) \tag{31.13}$$

The exponential temperature dependence derives from the Arrhenius temperature dependence of the rate constants describing the association and dissociation rate constants of the equilibrium particle association. These findings suggest that the clustering transition is controlled by the same mechanism as simple associating systems. This observation provides a framework for rationalizing the behavior of many nanoparticle systems, which should in turn aid in the control of dispersion and nanocomposite properties.

It is generally appreciated that highly asymmetric nanoparticles have the potential to be even more effective than spherical (or nearly spherical) nanoparticles in changing the properties of the polymer matrix to which they are added. In addition to the large enhancements in viscosity and shear modulus expected from continuum hydrodynamic and elasticity theories, extended nanoparticles can more easily form network structures both through direct interaction between the nanoparticles, or through chain bridging between the nanoparticles, where a "bridging" chain is a chain in contact with at least two different nanoparticles. These noncontinuum mechanisms are believed to play a significant role in property enhancement in polymer nanocomposites compared to more "classically" behaving microcomposites. An increase in viscosity with increasing number of particles, N, is expected from basic polymer physics, since the chain friction coefficient increases with N. Interchain interactions and "entanglement" interactions enhance this rate of increase, since the friction coefficient of each chain increases linearly with N. Computer simulations and experiments show that the origin of the increase must be more complex than simply increasing N.

We define a "bridging chain" as a chain that is simultaneously in contact with two or more nanoparticles. It was shown that the fraction of bridging chains, f_B,

increases with increasing N for every chain length. Hence, the fraction of bridging chains seems to be a useful "order parameter" for characterizing the polymer–nanoparticle interactions. If the polymer–nanoparticle interactions were sufficiently small, the bridging would not be expected to play significant role, and it is likely that the continuum hydrodynamic approach would be applicable. However, Sternstein and Zhu [73] and Kalfus and Jancar [75] have shown that for rubbery matrices, even in the case of weak NP–chain interaction, the chain stiffening can become enormous due to perturbation of entanglement mobility resulting in "trapped" entanglements.

31.4 TECHNOLOGIES FOR *ASSEMBLING* HIERARCHICAL COMPOSITE SUPERSTRUCTURES

The term *additive manufacturing* describes processes in which machine reads in the computer design and lays down successive layers of liquid or powder, and in this way builds up the 3D shape from a series of cross sections. These layers, which correspond to the virtual cross section from the computer model, are joined together or fused automatically to create the final shape. A number of competing technologies are available. They differ in the way layers are built to create parts, and the materials that can be used. Some methods use melting or softening material to produce the layers, e.g., *selective laser sintering* (SLS) and *fused deposition modeling* (FDM), while others lay liquid materials that are cured with different technologies, e.g., *stereolithography* (SLA). The current resolution of 3D printing process is in tens of micrometers, since the state-of-the-art printers use droplets 20–50 mm in diameter, although some technologies can produce layers as thin as 16 mm. Horizontal resolution equal to that for standard laser printers. Ultra-small features can be fabricated by the 3D microfabrication technique of *multiphoton* photopolymerization. In this approach, the desired 3D object is traced out in a block of gel by a focused laser. The gel is cured to a solid only in the places where the laser beam was focused, because of the *nonlinear* nature of photoexcitation, and then the remaining gel is washed away. Feature sizes of under 100 nm are easily produced, as well as complex structures such as moving and interlocked parts.

The *3D printing* technology was being studied for possible use in tissue engineering applications. Layers of living cells are deposited onto a gel medium or polysaccharide matrix and slowly built up to form three-dimensional structures including vascular systems. It was shown that it is possible to use 3D printing techniques to create chemical compounds, including new ones [118]. They first concept printed chemical reaction vessels, then use the printer to squirt reactants into them as "chemical inks" which then react producing new compounds to verify the validity of the process. Whilst most 3D printers are currently used for prototyping and in preproduction mold making processes, the use of 3D printing to manufacture end-use parts is also now occurring as *direct digital manufacturing* (DDM).

31.4.1 SELF-ASSEMBLY

Self-assembly (SA) in the classic sense can be defined as the spontaneous and reversible organization of NSBBs into ordered structures by noncovalent interactions. SA is a type of process in which a disordered system of pre-existing components forms an organized structure or pattern as a consequence of specific, local interactions among the components themselves, without external direction. The spontaneity of this process is the key property. In other words, the desired nanostructure builds itself. The SA processes most often take place on the *nanometer* and *micrometer* scales. DNA, proteins, lipid membranes, and other biological structures represent the natural examples of such organization. Important examples of SA in materials science include the formation of molecular crystals, colloids, lipid bilayers, phase-separated polymers, and self-assembled monolayers. Recently, the three-dimensional macroporous structure was prepared via SA of diphenylalanine derivative under cryoconditions; the obtained material can find the application in the field of regenerative medicine or drug delivery system.

The self-assembled structure must have a higher order than the isolated components, be it a shape or a particular task that the self-assembled entity may perform. Another distinctive feature of SA is that the building blocks are not only atoms and molecules, but span a wide range of nano- and mesoscopic structures, with different chemical compositions, shapes, and functionalities. Recent examples of novel building blocks include polyhedra and patchy particles. These NSBBs can in turn be synthesized through conventional chemical routes or by other SA strategies such as directional entropic forces (DEFs). Self-assembling NSBBs adopt a structure at the thermodynamic minimum, finding the best combination of interactions between subunits but not forming covalent bonds between them. Another characteristic common to nearly all self-assembled systems is their *thermodynamic stability*. For SA to take place without intervention of external forces, the process must lead to a lower Gibbs free energy, thus self-assembled structures are thermodynamically more stable than the single, unassembled components. A direct consequence is the general tendency of self-assembled structures to be relatively free of defects. Weak interactions and thermodynamic stability rationalize the *adaptability* to perturbations exerted by the external environment often found in self-assembled systems. Small fluctuations that alter thermodynamic variables can lead to marked changes in the structure and even compromise it, either during or after SA. The weak nature of interactions is responsible for the flexibility of the architecture and allows for rearrangements of the structure in the direction determined by thermodynamics. If fluctuations bring the thermodynamic variables back to the starting condition, the structure is likely to go back to its initial configuration. This leads the *self-healing* capability of self-assembled structures, which is generally not observed in materials synthesized by other techniques.

From what we have written so far, it should be evident that SA is a process which is easily influenced by external parameters: if this can make synthesis more problematic due to the many free parameters that require control, on the other hand it has

the exciting advantage that a large variety of shapes and functions on many length scales can be obtained [119]. Generally speaking, the fundamental condition needed for NSBBs to self-assemble into an ordered structure is the simultaneous presence of long-range repulsive and short-range attractive forces [120,121]. By choosing precursors with suitable physicochemical properties, it is possible to exert a fine control on the formation processes that produce complex structures. Clearly, the most important tool when it comes to designing a synthesis strategy for a composite structure is the knowledge of the chemistry of the building units. For example, it was demonstrated that it was possible to use diblock copolymers with different block reactivities in order to selectively embed specific nanoparticles and generate periodic nanocomposite with potential use as waveguides [122].

The main advantage of materials with hierarchical morphology is the ability to perform specific functions at a given length and time scale and the possibility to custom tailor these materials according to requirements of any particular application. Synthesis of chains with prescribed backbone structure using advanced polymerization of macromonomers represents one of the most promising directions in synthesis of polymers for engineering their assembly into desired supermolecular structures. Tethering of custom tailored polymers or oligomers onto surface of nanoparticles is considered the most efficient way to control nanoparticle SA allowing to obtain highly extended heterogeneous anizotropic superstructures even from spherical nanoparticles [110]. Transition from single structural scale heterogeneous materials, such as fibrous composites, to more sophisticated multiscale multifunctional heterogeneous materials with engineered interactions between the various structural levels similar to natural composites such as bones, cytoskeletons, shells, or wood, is just being considered. Ability to attach specific functions to particular structural scale can lead to the engineered control over the property and function development in the preparative stage mimicking the natural growth process synthetically. Research of the formation, stability, and properties of self-assembled nanostructured building blocks and the interactions between the various length scales in superstructures made of these blocks may prove decisive for future design of smart multifunctional heterogeneous polymeric materials for advanced engineering and biomedical applications.

Nanocomposites composed of BCPs and nanoparticles have attracted much attention because BCPs organize into diverse multiphase structures at various length scales with nanoscale periodicity and because of the recognition that the properties of even ordinary polymers can strongly benefit from the addition of nanoparticles [67]. It is believed that BCPs of various molecular structure represent the means to achieve control over the behavior of interfaces in the heterogeneous materials at the nanoscale and the SA creates possibility for the interscale signaling. Synthetic control over the BCP molecular structure allows developing superstructures in a prescribed manner. Novel heterogeneous polymeric materials prepared by copolymerizing and/or joining synthetic macromonomers or polymers with biopolymers or to form BCPs of organic and inorganic chains offer a promise to design materials possessing unheard of balance of properties and functions. This could result in completely new class of materials with improved biocompatibility, easier recycling,

and improved thermal resistance allowing to use these materials at higher operating temperatures. Moreover, combining polymers of vastly different nature may result in formation of nanostructures with useful engineering properties and biomedical functions.

A recurrent problem in the blending of BCPs and nanoparticles is the propensity of nanoparticles to self-assemble into extended clusters that can greatly affect the BCP ordering morphology and the very nature of the BCP order–disorder transition (ODT). Thermal fluctuations in BCP materials characteristically drive the ordering phase transition order from second to first order by the well-known Brazovskii mechanism and there have been many observations of jumps in X-ray and neutron scattering intensity data at the ODT that signal this phenomenon. This phenomenon offers both technological problems and opportunities. An infinitesimal amount of disorder can destabilize the first-order phase transition by transforming into some "glass-like" state where ordering is so frustrated that only a highly rounded remnant of the original phase transition then exists. It has been observed that the SA nanoparticles into extended structures can also serve as a template for the directed BCP assembly when the extended nanoparticle superstructures remain localized to the BCP microdomains, implying a synergistic interaction between the nanoparticle assembly and BCP ordering processes. These observations together suggest that the capacity of the clustered nanoparticles to span different BCP domains is important for disrupting the BCP ordering process. In this context, the suppression of the ordering process is a beneficial effect for polymer battery applications since crystallization leads to a drop of conductivity and battery function. The effective manipulation of this type of BCP organization can be expected to have application in the organic photovoltaic field, fuel cells, and bottom-up SA based fabrication processes utilizing BCP materials as templates.

There has been considerable interest in utilizing particle SA as a "bottom-up" route to new material assembly [11]. Such particle SA is of interest because it might, for example, allow us to construct improved polymer nanocomposites with "dialed-in" properties [14,123]. Our unique ability to control nanoparticle organization might, thus, allow us to build range of versatile bioinspired systems for an entirely new range of synthetic applications. It has also been shown that structural proteins such as collagen can undergo SA process resembling first-order thermodynamic transitions in forming microfibrils, which controls to a great extent the mineralization process to form basic building blocks of bones.

The extended nanoparticle structures can more easily form transient networks both through direct interaction between the nanoparticles or through chain bridging between the nanoparticles, where a "bridging" chain is a chain in contact with at least two different nanoparticles. These noncontinuum mechanisms are believed to play a significant role in property enhancement in polymer nanocomposites compared to more "classically" behaving microcomposites. The fraction of bridging chains seems to be a useful "order parameter" for characterizing the polymer–nanoparticle interactions. If the polymer–nanoparticle interactions were sufficiently small, the bridging would not be expected to play significant role, however, we have shown that the

chain stiffening can become enormous due to perturbation of entanglement mobility due to random nanoparticle packing resulting in "trapped" entanglements [73].

It has been suggested by many previous workers that nanoparticle shapes and their mutual interactions as well as interactions with chains determine the superstructures that they can assemble into [70,99,110]. The geometry of the assemblies is, thus, largely encoded at the level of a single nanoparticle. Similarly, flow effects can also be used to assemble particles into anisotropic structures [110]. Obtaining controlled dispersion of nanoparticles in polymer matrices is a significant challenge in achieving the dramatic property improvements promised by polymer nanocomposites [70]. However, it is often difficult to achieve this goal since inorganic particles are typically immiscible with an organic phase. One strategy to overcome this difficulty is to "shield" the particle surface by grafting it with the same chains at least partly miscible with the matrix polymer. While this approach for particle dispersion is successful in some cases, we find instead that the particles themselves can exhibit SA into highly anisotropic structures [110]. This process arises because the immiscible particle core and grafted polymer layer attempt to phase separate but are constrained by chain connectivity—this is evidently analogous to "microphase separation" in BCPs and other amphiphiles. Similar to these amphiphiles, these particles with a "polarizable" segmental cloud can self-assemble under a broad range of conditions into a variety of superstructures.

Drugs or diagnostic nanoparticles may be encapsulated, adsorbed, or dispersed in polymer nanostructures and the nanosize range of these delivery systems allows them to be injected directly into the systemic circulation without the risk of blocking blood vessels. Researchers have demonstrated that opsonization and subsequent recognition and phagocytosis by macrophages is strongly correlated with the size of the particle. Amphiphilic BCPs are able to form micelles, nanospheres, nanocapsules, and polymersomes [67]. The ability to conjugate biologically active ligands to the brush surface provides a further means for targeted therapy and imaging. Hence, polymersomes hold enormous potential as nanostructured biomaterials for future in vivo drug delivery and diagnostic imaging applications.

The fabrication of responsive/adaptive colloidal systems possessing quasi-stable organization, which can be tuned by an external signal, is a strong stimulus for research of polymer brushes on nanoparticles [110]. These systems are capable of switching their interfacial interactions in response to external signals due to a reversible change in their surface chemical composition and conformation. Recently, synthesis and characterization techniques for nanoparticles have rapidly developed, indicating the importance of organizing these particles into various assemblies to obtain novel properties that may arise from their 2D and 3D arrangements. The surface functionalization of nanoparticles by grafting specific polymer chains is expected to play important role in the designing of novel organic/inorganic smart nanocomposite coatings [124] and mass storage media [125].

The efficiency of photovoltaic devices is often limited by the short diffusion range of photogenerated charge carriers and the size of the active region corresponds to the diffusion range of photogenerated charge carriers, typically 10–20 nm [67,90].

Morphological differences, such as chain conformation or domain size, often overshadow the effect of charge transfer, so that device performance is not necessarily correlated with rapid decay times. It was found that the photoinduced electron transfer from semiconducting polymers onto C_{60} is reversible, ultrafast with a quantum efficiency approaching unity, and metastable. Doping of polymeric systems with fullerenes to form bulk heterojunctions resulting from the extended interfaces leads to efficient dissociation of the charge pairs generated under sunlight. The size reduction of the acceptor domains led to a complete quenching of the radiative recombinations. A simultaneous increase of the photocurrents could be achieved by the dispersion and size optimization of the nanofillers. The strong influence of the molecular morphology on the nanocomposite properties emphasizes the large improvements, which can still be gained on the performances of organic solar cells [67].

31.4.2 COMMANDED ASSEMBLY

While the self-assembling biocomposite systems rely on spontaneous organization of molecules and/or NPs, commanded/forced assembly (CA) approach used in state-of-the-art additive manufacturing needs well-controlled external driving stimulus [126]. CA processes employ external driving force to build a structure and/or prevent spontaneous structure disintegration. Another difference between *SA* and *CA* to material engineering is associated with the scale of the process. *Commanded assembly* cannot be usually performed effectively on the submicron scale and therefore it usually restricted to structures *above the micrometer size* [126].

Present commercial printers are capable to print conventional thermoplastics (PA, ABS), ceramics, low melting point metals, waxes, photocurable resins, etc. Recent research in this area focuses especially onto the development of various special materials for rapid prototyping and direct additive fabrication, such as graphene, electrically conductive composites, glass/HA powders, natural clay powders, calcium silicate ceramics, hydraulic setting $Mg_3(PO_4)_2$ powders, lead alloys, and many other materials.

The conventional 3D material printing can be hardly considered forced assembly, forced shaping would be probably a more adequate term. However, several interesting papers recently reported 3D printing of penetrating bi- or multimaterial objects with different levels of intermaterial mutual contact, which indeed exploit the forced assembly idea at the microlevel and manifest very interesting properties. A prominent group of reports focuses on the direct fabrication of articles associated with the life science sector, namely biocompatible scaffolds with potential medicinal application. Materials including poly(lactic acid)–HA composite, poly(lactic-co-glycolic acid) copolymer, hydroxyl-functionalized poly(e-caprolactone), or calcium phosphate have been successfully shaped into object of varying complexity, starting from simple cell aggregates, continuing through bone-like scaffolds and going up to aortic valves and biomimetic microvascular networks. The number of papers on nonbiologically targeted materials is rather scarcer, but yet several interesting outcomes have been reported, including cement and Al_2O_3 composites, Al_2O_3/CuO interpenetrating phase composite, negative index metamaterials for optical applications, and so on.

31.5 NANOSCALE BUILDING BLOCKS

Understanding must be achieved of the fundamental links between NSBB syntheses, hierarchical structure SA, properties and functions at multiple length *and* time scales requiring interdisciplinary approach integrating concepts and techniques from engineering, material science, structural biology, chemistry, and physics. Analysis of a broad range of hierarchical functional biomaterials and recent computer simulations demonstrated that the NSBBs' architecture can be used to encode simple design rules resulting in a unique self-assembled superstructures. A prerequisite to exploiting these NSBBs in assembly of functional composite hierarchies is to develop synthetic techniques to produce NSBBs and techniques that induce the NSBBs to self-assemble into target hierarchical structures in technologically plausible time scale. However, it is often difficult to achieve this goal since inorganic NPs are typically immiscible with an organic phase. One strategy to overcome this difficulty is to "shield" the NP surface by grafting it with the chains at least partly miscible with the matrix polymer. While this approach for NP dispersion is successful in some cases, it was found instead that the NPs themselves can exhibit SA into highly anisotropic structures. NPs with a "polarizable" segmental cloud can self-assemble under a broad range of conditions into a variety of substructures. Grafting of single or multiple chains of varying molecular weight onto single NP with different particle shape and properties is one of the routes to multifunctional NSBBs with prescribed supermolecular architecture. Grafting multiple NPs onto BCP chain or chain assembly, thus, forming extended nanoscale reinforcing elements or use NPs as temporary cross-links capable of joint recovery after breaking due to overloading has not been reported in the literature, yet.

31.5.1 SYNTHETIC NSBB PREPARATION

Group transfer polymerization (GTP), atom transfer radical polymerization (ATRP), reversible addition-fragmentation chain transfer polymerization (RAFT), ring-opening metathesis polymerization (ROMP) and ring-closing metathesis polymerization (RCM), acyclic diene metathesis (ADMET), and ring-expansion metathesis polymerization (REMP) are methods for synthesis of wide range of BCPs and functional macromonomers (FMMs) [127–129]. Utilizing these syntheses, polymers, interpenetrating polymer networks (IPNs), BCPs, and FMMs with controlled molar masses, well-defined macromolecular architectures, stereoregularity and small polydispersities can be prepared. ROMP is a superior method for making diblock and triblock BCPs. ADMET was used to prepare a series of "N-terminus" amino acid and peptide branched, chiral polyolefins termed *bio-olefins*. REMP can produce pure cyclic polyolefins containing a large quantity of double bonds in their main chain, providing a chemical handle for further modification, using methods like thiolene chemistry reducing oxygen inhibition, significantly. The thiolene chemistry can also produce polymer networks with delayed gelation, low levels of shrinkage, high conversions,

and uniform cross-linking densities, resulting in unique physical and mechanical properties [127].

It was shown that BCPs can organize into diverse multiphase structures at various length scales with nanoscale periodicity and it was recognized that the properties of even BCPs prepared from ordinary comonomers can strongly benefit from the addition of suitable NPs [23,27,107,108,127–138]. Grafting of single or multiple chains of varying molecular structure onto single NP with different particle shape and properties (POSS, CNT, graphene, etc.) is one of the promising routes to functional NSBBs with prescribed supermolecular architecture. The surface-initiated ATRP technique had been successfully used for the growing of well-defined homopolymers [128], diblock copolymers [127], graft copolymers, star polymers, and hyperbranched polymers from various NPs. Novel NSBBs were synthetized in our laboratory using ATRP from single reactive site POSS surface allowing better control over the molecular weight and molecular weight distribution of the target-grown PS and PMMA chains. Grafting multiple NPs onto precisely defined BCP chain or multiple chain assembly, thus, forming hybrid NSBBs or use NPs as temporary cross-links capable of joint recovery after breaking due to overloading has not been reported in the literature, yet. Assembly of 1D, 2D, and 3D supramolecular structures and interpenetrating networks (IPNs) with prescribed structure from NSBBs synthetized using advanced polymerization techniques represents one of the most promising directions in synthesis of polymers with desired supermolecular structure. Tethering of custom tailored BCPs or FMMs onto surface of NP, growing one or multiple chains from NP surface and grafting of multiple NPs along BCP chain are considered the most efficient in preparing hybrid NSBBs (HNSBBs) with encoded SA motives.

Amphiphilic BCPs have attracted a great deal of attention in terms of their ability to form various types of nanoparticles referred to as micelles, nanocapsules, nanospheres, core–shell nanoparticles, etc. [109,139–142]. BCP micelles are water soluble, biocompatible nanocontainers in the size of 10–100 nm, characterized by a core–shell architecture in which the core serves as a reservoir for the incorporation of poorly water soluble drugs, while the hydrophilic shell provides a protective interface between the core and the external medium. Synthesis and properties of amphiphilic BCPs that contain hydrophilic poly(ethylene glycol) (PEG) have gained much attention due to their specific physicochemical and biological properties. Biodegradable hydrophobic polymers such as polylactide (PLA), poly(DL-lactic-*co*-glycolic acid) (PLGA), poly(ε-caprolactone), and trimethylenecarbonate have been used mostly for the core material (lipophilic domain) of micelle to encapsulate a variety of therapeutic compounds. PLGA–PEG BCPs have shown usually quite microphase separation, crystallinity, and water solubility. These BCPs spontaneously assemble into a spherical micelle in aqueous environments. Drug release can be manipulated by choosing biodegradable polymers with different surface or bulk erosion rates, and external conditions such as pH and temperature changes may function as a switch to trigger drug release [142].

Grafting of single or multiple BCPs or FMMs onto single NP with different particle shape and properties (HAP, β-TCF, SiO_2, POSS, SWCNT, NT, SLG, CNC, etc.)

is the most effective route to NSBBs with prescribed supermolecular architecture. Alternatively, NSBBs can be formed by growing chains from the single NP surface after anchoring a suitable catalyst on it, which will be more precise, however, much less effective. Grafting multiple NPs onto BCP is the process intended for forming extended "mineralized" reinforcing elements (1D strings, 2D sheets, 3D networks). This has not been achieved synthetically in a precisely controlled manner, yet.

Within the past decades, the sol–gel process has been widely used in the *bottom-up* fabricating of novel organic–inorganic hybrid materials. In the case of composites, the goal is to carry out the sol–gel reaction in the presence of polymeric molecules and contain functional groups to improve their bonding to the inorganic phase [143]. This is a very useful novel reinforcement technique, which can generate reinforcing NPs within a polymer matrix. The sol–gel process surpasses the traditional blending method since it can subtly control the morphology or surface characteristics of the growing inorganic phase in the polymer matrix by control of these reaction parameters. Choice of base or acid catalyst controls both the process kinetics and the size of the resulting inorganic inclusions.

31.5.2 POSS-BASED NSBBS

POSSs [144] belong to a group of suitable inorganic NPs capable of forming inorganic "core" of the hybrid inorganic "core"–organic "shell" NSBBs due to their regular structure engineered at molecular level and controlled by their synthesis. It seems worthwhile to illustrate the strategies for synthetizing NSBBs using these well-defined systems. POSS substances form a diverse family of hybrid NPs with empirical formula $RSiO_{1,5}$, where R refers to an organic chemical moiety or hydrogen. POSS systems are known to exhibit different structures including random structure, ladder structure, cage structures, and partial cage structure, as illustrated in Figure 31.2.

POSS particles consist of a silica core cage $(SiO_{1,5})_n$ with $n = 8$, 10, 12 and external organic substituents, which could be represented by any chemical group known in organic chemistry. Different substituents could be present in one molecule, which results in huge number of available POSS variants. This variability together with the POSS well-defined structure compared to nanosilica attracts wide attention of scientists. Nowadays, more than 80 different POSS types including alkyls, olefins, alcohols, esters, anhydrides, acids, amines, imides, epoxies, thiols, sulfonates, fluoroalkyls, silanols, and siloxides are commercially available [145–147].

31.5.3 POSS SYNTHESIS

In general, the classical synthetic approach involves a hydrolysis of trifunctional organo- or hydrosilanes [148]. Silsesquioxane $(HSiO_{1,5})_n$ represents the simplest member of the class and it could be employed as a precursor for variety of POSS-type preparation. It was first synthesized unintentionally by Müller and coworkers in 1959 from trichlorosilane by hydrolysis with sulfuric acid. Frye and Collins developed a

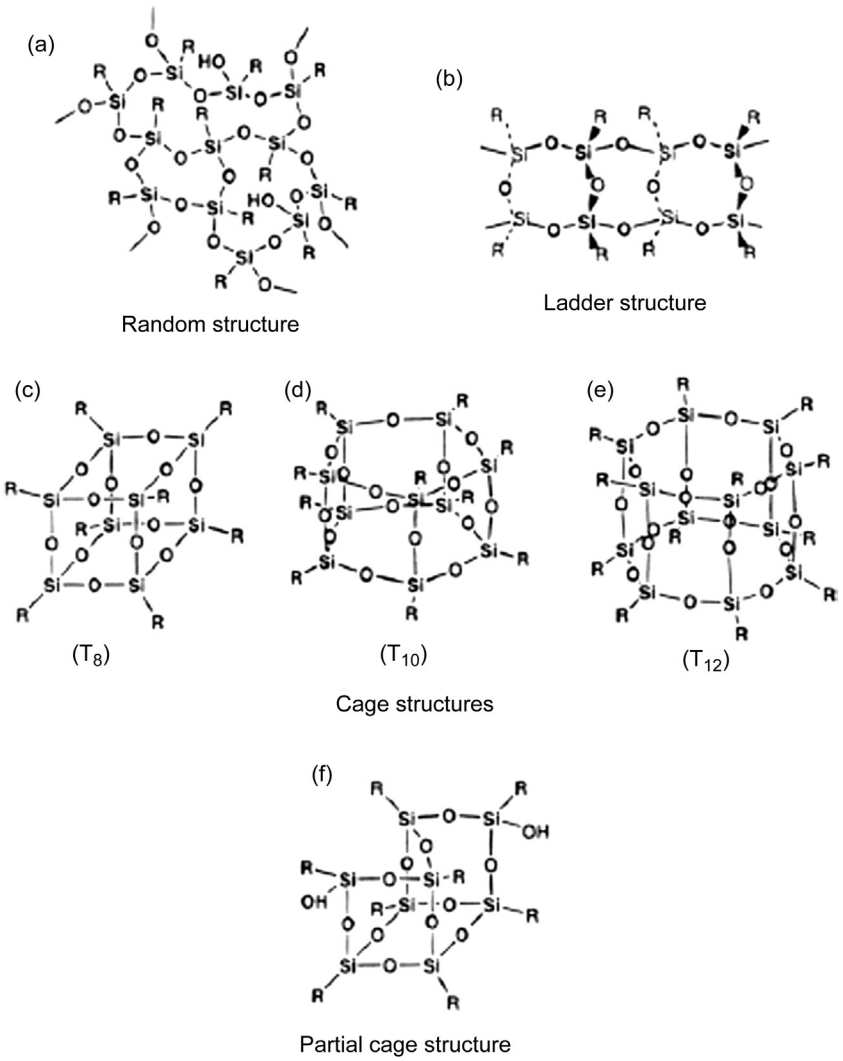

FIGURE 31.2

Structures of silsesquioxan [144].

new process by hydrolysis of trimethoxysilane [149] and Agaskar [150] introduced a new method by hydrolysis of trichlorosilane in scarce-water conditions.

Three approaches were reported to synthesize mono- and multifunctional POSS. Cohydrolysis of monomers with different organic moieties (*R* and *R*') leads to a mixture of products with all possible *R*/*R*' ratios, therefore further separation is necessary in order to receive pure substances. Various methods based on substitution reactions

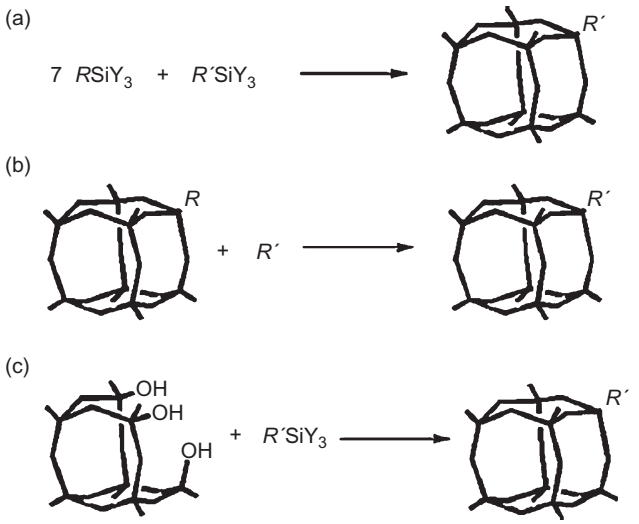

FIGURE 31.3

Methods of monofunctional POSS synthesis: (a) cohydrolysis of different monomers, (b) substitution reaction, and (c) corner capping reaction.

with retention of the siloxane cage were described, e.g., hydrosilation of the basic hydrido-T_8 unit. The last approach is commonly referred as a corner capping reaction which was first reported by Brown and Vogt [148] and further improved by Feher and Lichtenhan [93,151] and it is represented by a reaction of monomer with incompletely condensed (T_7) molecules; however, long reaction times and diversity limitations are the major disadvantages of this technique. The methods of monofunctional POSS synthesis are schematically summarized in Figure 31.3, where *Y* represents a silane functional group.

31.5.4 POSS PROPERTIES

Polyhedral silsesquioxanes (POSS) unique properties origin in its hybrid organic–inorganic structure and predominantly depend on its R substituents attached to the inorganic core [152–154] including its compatibility and solubility in solvents. POSS are mostly solid white powders and some are colorless liquids. The powder particles possess diameter typically between 1 and 100 microns; however, in solvents POSS forms entities ranging from 1–3 nm to micron-sized domains according to its compatibility with the specific solvent. POSS nanostructures can be considered as the smallest possible particles of silica; however, despite its common reference as molecular silica, POSS have lower densities (0.97–1.82 g/cm^3 compared to 2.60 g/cm^3 of quartz) and are less abrasive with Mohs hardness of approximately 1.

Unlike many organic compounds, POSS are nonvolatile, odorless, and environmentally friendly substances. Their acute oral toxicity belongs to the lowest category

both in the European Union ($LD_{50} \leq 2000$ mg/kg pursuant to the Regulation (EC) 1272/2008) and in the United States ($LD_{50} \leq 5000$ mg/kg pursuant to the Toxic Substances Control Act) regarding to the performed toxicity tests; however, results are not available for all types of POSS and further testing is being carried out.

31.5.5 POSS IN POLYMERS

POSS additives dedicated to polymeric materials are available on commercial scale. Hybrid Plastics' manufacturing facility manages capacity in the hundreds of metric tons per year range. POSS substituents on their surface could be tailored to provide miscibility with most polymers without any further surface treatment; however, a fundamental description of nonequilibrium POSS nanoparticles' SA and its influence on a polymeric matrix on the molecular scale remains a riddle. In addition, POSS could be physically blended in a polymeric matrix as common fillers by solution or melt blending or covalently bonded to a polymer chain through reactive functional groups what consequents to several POSS/polymer architectures as shown in Figure 31.4.

Tuning the POSS substituents is a well-established method in tailoring the POSS/polymer nanocomposite properties with close impact to miscibility and dispersion state of the nanoparticles. Blends with fully dispersed nanoparticles at a molecular scale as well as POSS domain formation of various sizes were reported [152–154] and the diversity is further pronounced by existence of both crystalline [155–157] and amorphous nature of the domains [158,159].

Kuo and Chang investigated an influence of hydrogen bonding on miscibility between POSS core and phenolic group on model compounds octaisobutyl-POSS and 2,4-dimethylphenol. The free energy of mixing two polymers ΔG_m could be expressed by Flory–Huggins equation with Painter and Coleman supplement [158] which accounts the free energy of hydrogen bond formation contribution ΔG_H:

$$\frac{\Delta G_m}{RT} = \frac{\phi_A}{M_A}\ln\varphi_A + \frac{\phi_B}{M_B}\ln\varphi_B + \phi_A\phi_B\chi_{AB} - \frac{\Delta G_H}{RT} \tag{31.14}$$

where ϕ_A and ϕ_B are volume fractions of the polymers, M_A and M_B are the corresponding degrees of polymerization, and χ_{AB} denotes the interaction parameter. By employing the Coggeshall and Saier equation:

$$K_a = \frac{1 - f_m^{OH}}{f_m^{OH}(C_A - (1 - f_m^{OH})C_B)} \tag{31.15}$$

where K_a is the equilibrium constant for the hydrogen bond association, C_A and C_B are the concentrations (in mol/L) and f_m^{OH} is the fraction of free bond-donating group, which is built in the Painter–Coleman association model [158]. Kuo and Chang

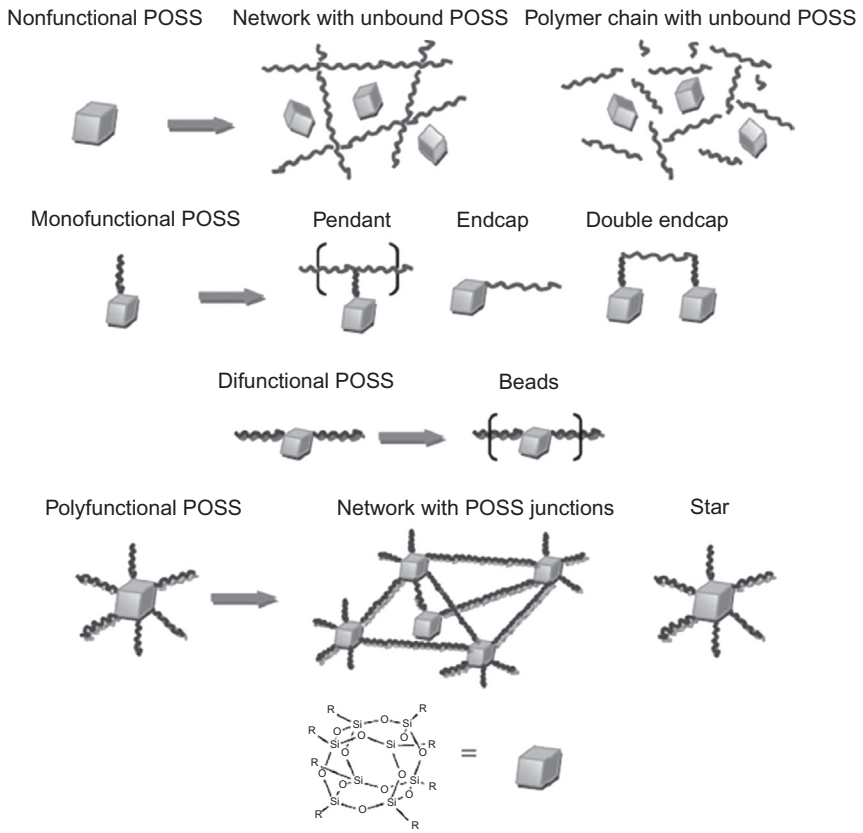

FIGURE 31.4

POSS/polymer architectures.

estimated that Novalic type phenolic resin self-association equilibrium constant (52.3) exceeds the equilibrium constant of hydrogen bond formation between phenolic OH group and POSS Si–O–Si group (38.7). Despite its positive contribution, the hydrogen bonding between POSS core and phenolic resin provides only partially miscible or immiscible mixtures and hydrogen bond accepting substituents are necessary to enhance the POSS-phenolic miscibility.

31.5.6 NSBB SELF-ASSEMBLY

So far, mostly computer simulations were used to demonstrate that the resulting anisotropy of the NSBBs' shape can be used to encode simple design rules into the NSBBs supramolecular architecture that ultimately result in a unique self-assembled superstructure. A prerequisite to exploiting these NSBBs is to develop synthetic techniques to produce NSBBs and techniques that induce the NSBBs to self-assemble into target

structures possessing the necessary properties or functionalities. Also here it can be found that inducing SA in NSBBs results in similar structures as mentioned already for NPs in section 31.3.3 [26]. The research in the area of mechanics of composites built using precisely designed synthetic NSBBs is still in its infancy, mostly due to synthetic difficulties. Moreover, no theoretical framework has been published describing the laws governing multi length scale assembly of NSBBs consisting of BCPs, supramolecular amphiphiles (SMAs), functionalized macromonomers (FMMs), hybrid block copolymers (HBCPs), hybrid nanoparticle amphiphiles (HNPAs), or chain decorated NPs into hierarchical superstructures [70,110,127,128,159].

In computer simulations, surface functionalized NPs are typically represented as patchy particles, where patch represents certain chemical groups responsible for interactions. The most well-studied case is Janus particles [160] (JPs), named after roman god with two faces. JPs have two parts with different chemical properties, originally both parts had the same size, but lately also particles with asymmetric parts have started to be called Janus particles. Spherical symmetric JPs are able to form micelles and bilayers that can enclose themselves into a vesicle and a clear gas liquid coexistence region has been identified for these systems. Adding a charge to amphiphillic elipsoidal particles, more complex cluster structures can be obtained reflecting motifs related to the spatial distribution of the charge [161–166].

Nonsphericity of NPs adds additional parameter to explore and it has been shown that even simple repulsive rigid rods order upon increased density with riche phase diagram, which include nematic and smectic phases depending on the aspect ratio. Using more complicated shapes of polyhedra and faced spheres recent simulations demonstrated that nonspherical shape can support the SA and the facets give origin to entropic attraction in order of a few kT at intermediate densities (about 50%). The shape is also responsible for complex hierarchical SA of octapod structures investigated by both simulations and experiment. Combination of asymmetric shape with a patch character can result in Janus cylinders and discs, which can form not only micelles and bilayers, but also well-defined fibrils of two to four particles in cross section and sandwich structures. When patch is distributed only at the end of cylinders, “matchstick” aggregates were observed in well-defined multipods (dimers, star trimers, and star and tetragonal tetramers).

Naturally, self-assembling particles can have more interaction patches and such increased complexity leads to richer parameter space and morphologies to explore. Computer simulations have proven to be a useful tool in guiding experiments and pointing down important regions of the wide parameter space. Due to long-time scales necessary to see spontaneous assembly in the simulations the field is dominated by coarse-grained models, which reduce the complexity of the problem by averaging out unimportant degrees of freedom. Such models keep important physical features and allow us to study reasonable size and time scales required for investigation of equilibrium and/or kinetic properties of the system. Importantly, various chemical systems have been found in agreement with simulation findings including functionalized NPs, BCPs, dendrimers, and peptide coiled-coils similar to collagen triple helix [70,71]. This demonstrates that simulation results with coarse-grained

models can have various chemical realizations and as long as the model is describing the interactions accurately the self-assembled morphologies are the same.

For systems with more patches only few pioneering simulations has been carried out and those are focused on spherical NPs. Highly symmetric patch distribution may have different macroscopic phases including vapor, crystal, and liquid, where liquid phase can go to extremely low densities forming breached networks called empty liquids. Once the interaction sites are asymmetric, compact clusters of various sizes may occur. Moreover, kinetic study on these particles showed that bond distribution in each time frame of gelation can be related to equilibrium distribution at specific temperature. Therefore, the kinetic/aging process can be mapped on the cooling process in the equilibrium phase diagram.

31.6 CONCLUSIONS

The main challenge for the research and engineering of functional composite structures is to develop *novel* material platforms by revealing combined physicochemical routes to precisely supermolecularly designed NSBBs with *built-in* stimuli responsiveness, to discover processes for quick *bottom-up* assembly of hierarchical composite superstructures utilizing *SA* of NSBBs into micrometer-sized substructures followed by their computer-aided multi length scale 3D *forced assembly* into mesoscopic superstructures with prescribed structural and functional hierarchy and mechanochemical inter length scale signaling. This research to be successful should combine efforts from synthetic chemists preparing desired NSBBs and reactions for quick setting of self-assembled submicrometer assemblies, polymer physicists to develop theories describing mechanisms and kinetics of NSBB SA in relation to their shape and functionality, materials and process engineers to develop multi length scale composite fabrication technologies. Novel experimental techniques providing reliable data on structure and properties at multiple length and time scales should be developed to obtain structural data, properties, and functions simultaneously, critical for holistic understanding of the structure–property–function relationships in polymer composite *materiome*.

Further, novel theoretical models should be developed for quantitative relationships between structural variables, nature and kinetics of the hierarchy formation, and the physicochemical properties and functions of hierarchical composite superstructures. Obtaining theoretical description of the sequential assembly mechanisms providing structural and functional hierarchy of composite superstructures on various dimensional and time scales including inter length scale signaling, obtaining quantitative structure–property–function relationships in the various substructures and development of procedures for engineering properties and functions of these materials in the process of their preparation is an imminent challenge. Algorithms for computer-aided 3D assembly of NSBBs into 3D microscopic superstructures with prescribed structural and functional hierarchy should be developed considering sequential combination of fast localized SA followed by fixing these structures with

quick formation of chemical and physical bonds. Understanding the processes of nano- and micro length scale hierarchical structure formation with forced assembly capable of producing macroscopic 3D structures is envisioned as the technological paradigm of the twenty-first century fabrication of composite superstructures for both engineering and medical applications.

REFERENCES

[1] Cranford S, Buehler MJ. [Chapter 4] Biomateriomics. Springer; 2012. p. 399–424.
[2] Buehler MJ, Keten S. Nano Res 2008;1:63–71.
[3] Buehler MJ, Keten S, Ackbarow T. Prog Mater Sci 2008;53:1101–241.
[4] Cranford S, Buehler M. Nanotechnol Sci Appl 2010;3:127–48.
[5] Omenetto FG, Kaplan DL. Science 2010;329:528–31.
[6] Fratzl P, Weinkamer R. Prog Mater Sci 2007;52:1263–344.
[7] Vollrath F. Nature 2010;466:319.
[8] Aizenberg J, Weaver JC, Thanawala MS, Sundar VC, Morse DE, Fratzl P. Science 2005;309:275–8.
[9] Fratzl P. J Roy Soc Interface 2007;4:637–42.
[10] Studard AR. Adv Mater 2012;24:5024–44.
[11] Shenhar R, Norsten TB, Rotello VM. Adv Mater 2005;17:657.
[12] Patra TK, Singh JK. J Chem Phys 2013;138:144901.
[13] Mackay ME, Tuteja A, Duxbury PM, Hawker CJ, Van Horn B, Guan ZB, et al. Science 2006;311:1740.
[14] Starr FW, Douglas JF, Glotzer SC. J Chem Phys 2003;119:1777.
[15] Van Workum K, Douglas JF. Phys Rev E 2006;73:031502.
[16] Rabani E, Reichman DR, Geissler PL, Brus LE. Nature 2003;426:271.
[17] Gupta S, Zhang QL, Emrick T, Balazs AC, Russell TP. Nat Mater 2006;5:229.
[18] Ritchie RO, Buehler MJ, Hansma P. Phys Today 2009;62:41–7.
[19] Saffer EM, Tew GN, Bhatia SR. Curr Med Chem 2011;18:5676.
[20] Nakanishi T, Naffakh M, Díez-Pascual AM. J Phys Conf Ser 2009;159:012005.
[21] Marco C, Ellis GJ, Gómez-Fatou MA. Prog Polym Sci 2013;38:1163.
[22] Buehler MJ, Yung YC. Nat Mater 2009;8:175–88.
[23] Taylor D, HJG, Lee TC. Nat Mater 2007;6:263–6.
[24] Ji B, Gao H. J Mech Phys Solids 2004;52:1963–90.
[25] Wiener S, Wagner HD. Annu Rev Mater Sci 1998;28:271–98.
[26] Kreplak L, Fudge D. Bioessays 2007;29:26–35.
[27] Liu W, Jawerth LM, Sparks EA, Falvo MR, Hantgan RR, et al. Science 2006;313:634.
[28] Luz GM, Mano JF. Comp Sci Technol 2010;70:1777.
[29] Daniel IM, Abot JL, Schubel PM, Luo JJ. Exp Mech 2012;52:37.
[30] Kobayashi S. Compos B Eng 2012;43:1720.
[31] Ozcan S, Filip P. Wear 2005;259:642.
[32] Tong L, Mouritz AP, Bannister M. 3D fiber reinforced polymer composites. Amsterdam: Elsevier; 2002.
[33] Qian H, Greenhalgh ES, Schaffer MSP, Bismarck A. J Mater Chem 2010;20:4751.
[34] Veedu VP, Cao AY, Li XS, Ma KG, Soldano C, Kar S, et al. Nat Mater 2006;5:457.

[35] Ramanathan T, Abdala AA, Stankovich S, Dikin DA, Herrera-Alonso M, Piner RD, et al. Nat Nanotechnol 2008;3:327.
[36] Shin MK, Lee B, Kim SH, Lee JA, Spinks GM, et al. Nat Commun 2012;3:650.
[37] Stankovich S, Dikin DA, Dommett GHB, et al. Nature 2006;442:282.
[38] Espinoza HD, Rim JE, Barthelat F, Buehler MJ. Prog Mater Sci 2009;54:1059.
[39] Bruet BJF, Song JH, Boyce MC, Ortiz C. Nat Mater 2008;7:748.
[40] Jungnikl K, Goebbels J, Burgert I, Fratzl P. Trees Struct Func 2009;23:605.
[41] Elbaum R, Zaltzman L, Burgert I, Fratzl P. Science 2007;316:884.
[42] Fratzl P, Elbaum R, Burgert I. Faraday Discuss 2008;139:275.
[43] Pokroy B, Kang SH, Mahadevan L, Aizenberg J. Science 2009;323:237.
[44] Wong TS, Kang SH, Tang SKY, Smythe EJ, Hatton BD, Grinthal A, et al. Nature 2011;477:443.
[45] Bhushan B. Langmuir 2012;28:1698.
[46] Van Opdenbosch D, Fritz-Popovski G, Paris O, Zollfrank C. J Mater Res 2011;26:1193.
[47] Kim YY, Ganesan K, Yang PC, Kulak AN, Borukhin S, Pechook S, et al. Nat Mater 2011;10:890.
[48] Li HY, Xin HL, Muller DA, Estroff LA. Science 2009;326:1244.
[49] Junginger M, Bleek K, Kita-Tokarczyk K, Reiche Shkilnyy A, et al. Nanoscale 2010;2:2440.
[50] Dong Q, Su H, Cao W, Han J, Zhang D, Guo Q. Mater Chem Phys 2008;110:160.
[51] Pimenta S, Pinho ST. J Mech Phys Solids 2013;61:1337.
[52] Libanori L, Münch FHL, Montenegro DM, Studard AR. Comp Sci Technol 2012;72:435.
[53] Diéz-Pascual AM, Naffakh M, Marco C, Gómez-Fatou MA, Ellis GJ. Prog. Mater Sci 2012;57:1106–90.
[54] Khan SU, Kim JK. J Aeronaut Space Sci 2011;12:115.
[55] Gojny FH, Wichmann MHG, Fiedler B, Bauhofer W, Schulte K. Compos A Appl Sci Manuf 2005;36:1525.
[56] Qiu JJ, Zhang C, Wang B, Liang R. Nanotechnology 2007;18:275708.
[57] Rahmanian S, Thean KS, Suraya AR, Shazed MA, Salleh MAM, Yusoff HM. Mater Des 2013;43:10.
[58] Garcia EJ, Hart AJ, Wardle BR, Yamamoto M. Comp Sci Technol 2008;68:2034.
[59] Quian H, Greenhalgh ES, Shaffer MSP, Bismarck A. J Mater Chem 2010;20:4751.
[60] Bekyarova E, Thostenson ET, Yu A, Kim H, Gao J, Tang J, et al. Langmuir 2007;23:3970.
[61] Abot JL, Song Y, Schulz MJ, Shanov VN. Comp Sci Technol 2008;68:2755.
[62] Barber AH, Zhao Q, Wagner HD, Baillie CA. Comp Sci Technol 2004;64:1915.
[63] Warrier A, Godara A, Roches O, Meyyo L, Luiyi F, et al. Compos A Appl Sci Manuf 2010;41:532.
[64] Naffagh M, Díez-Pascual AM, Marco C, Ellis GJ, Gómez-Fatou MA. Prog Polym Sci 2013;38:1163.
[65] Zidek J, Kucera J, Jancar J. Computers Materials and Continua 2011;24:183–208.
[66] Jancar J, Fiore K. Polymer 2011;52:5851.
[67] Jancar J, Douglas JF, Starr FW, Kumar SK, Cassagnau P, Lesser AJ, et al. Polymer 2010;51:3321–43.
[68] Jancar J. Karger-Kocsis J, Fakirov S, editors. Nano- and micro-mechanics of polymer blends and composites. Hanser; 2009. p. 241–66.
[69] Jancar J, Hoy RS, Jancarova E, Lesser AJ, Zidek J. Macromolecules 2013;46:9409.

[70] Akcora P, Liu H, Kumar SK, Moll J, Li Y, Benicewicz BC, et al. Nat Mater 2009;8:354–9.
[71] Glotzer SC, Horsch MA, Iacovella CR, Zhang Z, Chan ER, Zhang Xi. Curr Opin Colloid Interface Sci 2005;10:287–95.
[72] Chabert E, Bornert M, Bourgeat-Lami E, Cavaillé J-Y, Dendievel R, et al. Mater Sci Eng A 2004;381:320.
[73] Sternstein SS, Zhu AJ. Macromolecules 2002;35:7262–73.
[74] Kalfus J, Jancar J. Comp Sci Technol 2008;68:3444–7.
[75] Kalfus J, Jancar J. J Polym Sci Polym Phys 2007;45:1380–88.
[76] Kalfus J, Jancar J. Polym Compos 2007;28:365–71.
[77] Riggleman RA, Toepperwein G, Papakonstantopoulos GJ, Barrat J-L, de Pablo JJ. J Chem Phys 2009;130:244903.
[78] Lin A, Meyers MA. Mater Sci Eng A 2005;390:27–41.
[79] Fantner GE, Oroudjev E, Schitter G, Golde LS, Thurner P, Finch MM, et al. Biophys J 2006;90:1411–8.
[80] Hansma PK, Fantner GE, Kindt JH, Thurner PJ, Schitter G, Turner PJ, et al. J Musculoskelet Neuronal Interact 2005;5:313–15.
[81] deGennes PG. Scaling concepts in polymer physics. Ithaka: Cornell University Press; 1979.
[82] Zheng X, Sauer BB, van Alsten JG, Schwarz SA, Rafailovich MH, Sokolov J, et al. Phys Rev Lett 1995;74:407.
[83] Lin YH. Macromolecules 1984;17:2846.
[84] Jancar J, Kucera J, Vesely P. J Mater Sci Letters 1988;7:1377.
[85] Chao H, Riggleman RA. Polymer 2013;54:5222.
[86] Arumugan P, Xu H, Srivastava S, Rotello VM. Polym Int 2007;56:461.
[87] Jancar J, Recman L. Polymer 2010;51:3826.
[88] Riggleman RA, Douglas JF, de Pablo JJ. Soft Matter 2010;6:292.
[89] Zhu A, Sternstein SS. Comp Sci Technol 2003;63:1113.
[90] Maranganti R, Sharma P. Phys Rev Lett 2007;98:195504.
[91] Boyd RH, Smith GD. Polymer dynamics and relaxation. Cambridge: Cambridge University Press; 2007. [Chapter 8.2].
[92] Richter D, Monkenbusch M, Arbe A, Colmenero J. Adv Polym Sci 2005;174:1–221.
[93] Lichtenhan JD, Vu NQ, Carter JA, Gilman JW, Feher FJ. Macromolecules 1993;26:2141–2.
[94] Schäfer BM, Hecht J, Harting A, Nirschl H. J Colloid Interface Sci 2010;349:186–95.
[95] Torquato S, Jiao Y. Phys Rev E 2012;86:011102.
[96] Molina-Bolívar JA, Galisteo-Gonzáles F, Hidalgo-Alvarez R. Colloids Surf B Biointerfaces 1999;14:3–17.
[97] Hooper JB, Schweizer KS. Macromolecules 2006;39:5133.
[98] Hooper JB, Schweizer KS. Macromolecules 2007;40:6998.
[99] Anderson BJ, Zukoski CF. Langmuir 2010;26:8709–20.
[100] Rahedi AJ, Douglas JF, Starr FW. J Chem Phys 2008;128:024902.
[101] Tantishaiyakul V, Worakul N, Wongpoowarak W. Int J Pharm 2006;325:8–14.
[102] Kim SY, Zukoski CF. Langmuir 2011;27:10455–63.
[103] Kalra V, Escobedo F, Joo YL. J Chem Phys 2010;132:024901.
[104] Glotzer SC, Coniglio A. Comput Mater Sci 1995;4:325.
[105] Torquato S, Hyun S, Donev A. J Appl Phys 2003;94:5748.
[106] Torquato S, Hyun S, Donev A. Phys Rev Lett 2002;89:26.

[107] Hyde ST, de Campo L, Oguey C. Soft Matter 2009;5:2782–94.
[108] Kirkensgaard JJK, Hyde S. Phys Chem Chem Phys 2009;11:2016–22.
[109] Yang Q, Tian J, Hu MX, Xu ZK. Langmuir 2007;23:6684–90.
[110] Kumar SK, Jouault N, Benicewicz B, Neely T. Macromolecules 2013;46:3199.
[111] Yan L-T, Xie X-M-. Prog Polym Sci 2013;38:369.
[112] Liu J, Gao Y, Cao D, Zhang L, Guo Z. Langmuir 2011;27:7926.
[113] Goswami M, Sumpter BG. Phys Rev E 2010;81:041801.
[114] Frishknecht AL, McGarrity ES, Mackay ME. J Chem Phys 2010;132:204901.
[115] Füllbrandt M, Purohit PJ, Schönhals A. Macromolecules 2013;46:4626.
[116] Liu J, Wu S, Zhang L, Wang W, Cao D. Phys Chem Chem Phys 2011;13:518.
[117] Riggleman RA, Toepperwein G, Papakonstantopoulos GJ, Barrat GL, dePablo JJ. J Chem Phys 2009;130:244903.
[118] Symes MD, et al. Nat Chem 2012;4:349–54.
[119] Lehn JM. Science 2002;295:2400.
[120] Forster PM, Cheetham AK. Angew Chem Int Ed 2002;41:457.
[121] Ariga K, Hill JP, Lee MV, Vinu A, Charvet R, Acharya S. Sci Technol Adv Mater 2008;9:014109.
[122] Gazit O, Khalfin R, Cohen Y, Tannenbaum R. J Phys Chem C 2009;113:576.
[123] Damasceno PD, Engel M, Glotzer S. Science 2012;337:453.
[124] Chau JLH, Hsieh C-C, Lin Y-M, Li A-K. Prog Org Coatings 2008;62:436–9.
[125] Griffiths RA, Williams A, Oakland C, Roberts J, Vijayaraghavan A, Thomson T. J Phys D Appl Phys 2013;46:503001.
[126] Li M, Ishihara S, Ji Q, Akada M, Hill JP, Ariga K. Sci Technol Adv Mater 2012;13:053001.
[127] Kumar SK, Krishnamoorti R. Annu Rev Chem Biomol Eng 2010;1:37–58.
[128] Bajpai AK, Shukla SK, Bhanu S, Kankane S. Prog Polym Sci 2008;33:1088–118.
[129] Zhang K, Lackey MA, Cui J, Tew GN. J Am Chem Soc 2011;133:4140–8.
[130] Michlovská L, Vojtová L, Mravcová L, Hermanová S, Kučerík J, Jancar J. Macromol Symp 2010;295:119–24.
[131] Vojtová L, Jancar J. Chemicke Listy 2005;99:491–2.
[132] Smrtka O, Jancar J. Chem Pap 2009;62:504–8.
[133] Morinaga T, Ohkura M, Ohno K, Tsujii Y, Fukuda T. Macromolecules 2007;40:1159–64.
[134] Park JT, Koh JH, Koh JK, Kim JH. Appl Surf Sci 2009;255:3739–44.
[135] Li L, Yan GP, Wu JY, Yu XH, Guo QZ, Kang ET. Appl Surf Sci 2008;255:7331–5.
[136] Xu C, Wu T, Batteas JD, Drain CM, Beers KL, Fasolka MJ. Appl Surf Sci 2006;252:2529–34.
[137] Riess Jean G. Curr Opin Colloid Interface Sci 2009;14:294–304.
[138] Krafft MP, Riess JG. Chem Rev 2009;109:1714–92.
[139] Liu P, Wang TM. Ind Eng Chem Res 2007;46:97–102.
[140] Hong CY, Zou YZ, Wu D, Liu Y, Pan CY. Macromolecules 2005;38:2606–11.
[141] Chen JC, Luo WQ, Wang HD, Xiang JM, Jin HF, et al. Appl Surf Sci 2010;256:2490–5.
[142] Rijcken CJ, Soga O, Hennink WE, van Nostrum CF. J Control Release 2007;120:131–48.
[143] Kuo S-W, Chang F-C. Prog Polym Sci 2011;36:1649–96.
[144] Baney M, Itoh M, Sakakibara A, Suzuki T. Chem Rev 1995;95:1409–30.
[145] Marcolli C, Calzaferri G. Appl Organometal Chem 1999;13:213–26.
[146] Tsuchida A, Bolln C, Sernetz FG, Frey H, Mülhaupt R. Macromolecules 1997;30:2818–24.
[147] Day VW, Klemperer WG, Mainz VV, Millar DM. J Am Chem Soc 1985;107:8262–4.

[148] Brown JF, Vogt LH. J Am Chem Soc 1965;87:4313–7.
[149] Frye CL, Collins WT. J Am Chem Soc 1970;92:5586–8.
[150] Agaskar PA. Inorg Chem 1991;30:2707–8.
[151] Feher FJ, Budzichowski TA, Rahimian K, Ziller JW. J Am Chem Soc 1992;114:3859–66.
[152] Phillips SH, Haddad TS, Tomczak SJ. Curr Opin Solid State Mater Sci 2004;8:21–9.
[153] Misra R, AlidedeoglU AH, Jarrett WL, Morgan SE. Polymer 2009;50:2906–18.
[154] Sánchez-Soto M, Schiraldi DA, Illescas S. Eur Polym J 2009;45:341–52.
[155] Fina A, Tabuani D, Frache A, Camino G. Polymer 2005;46:7855–66.
[156] Jeon HG, Mather PT, Haddad TS. Polym Int 2000;49:453–7.
[157] Perrin FX, Panaitescu DM, Frone AN, Radovici C, Nicolae C. Polymer 2013;54:2347–54.
[158] Coleman M, Painter P. Prog Polym Sci 1995;20:1–59.
[159] Iyer S, Schiraldi DA. Macromolecules 2007;40:4942–52.
[160] Yan L-T, Xie X-M. Prog Polym Sci 2013;38:369–405.
[161] Kowalewska A, Fortuniak W, Chojnowski J, Pawlak A, Gadzinowska K, Zaród M. Silicon 2012;4:95–107.
[162] Cui F-Z, Li Y, Ge J. Mater Sci Eng R 2007;57:1–27.
[163] Hartgering JD, Beniash E, Stupp SI. Science 2001;294:1684–8.
[164] Lutsko JF, Basios V, Nicolis G, Caremens TP, Aerts A, Martens JA, et al. J Chem Phys 2010;132:164701.
[165] Takenaka M, Hasegawa H. Curr Opin Chem Eng 2013;2:88–94.
[166] Toksoz S, Mammadov R, Tekinay AB, Guler MO. J Colloid Interface Sci 2011;356:131–7.
[167] Kutvonen A, et al. J Chem Phys 2012;137:214901.